EXPERRIMENTAL ASSESSMENT OF EFFECT OF INTERMEDIATE PRINCIPAL STRESSES ON ROCK TENSILE STRENGTH

Pakpoom Poonprakon

A Thesis Submitted in Partial Fulfillment of the Requirements for the Degree of Master of Engineering in Geotechnology

Suranaree University of Technology

Academic Year 2009

การทดสอบผลกระทบของความเค้นหลักกลางต่อค่ากำลังดึงของหิน

นายภาคภูมิ พูนประโคน

วิทยานิพนธ์นี้เป็นส่วนหนึ่งของการศึกษาตามหลักสูตรปริญญาวิศวกรรมศาสตรมหาบัณฑิต
สาขาวิชาเทคโนโลยีธรณี
มหาวิทยาลัยเทคโนโลยีสุรนารี
ปีการศึกษา 2552

EXPERIMENTAL ASSESSMENT OF EFFECT OF INTERMEDIATE PRINCIPAL STRESSES ON ROCK TENSILE STRENGTH

Suranaree University of Technology has approved this thesis submitted in partial fulfillment of the requirements for the Master's degree.

Thesis Examining Committee

_____

(Asst. Prof. Thara Lekuthai)

Chairperson

_____

(Assoc. Prof. Dr. Kittitep Fuenkajorn)

Member (Thesis Advisor)

_____

(Dr. Prachaya Tepnarong)

Member

_____

(Prof. Dr. Pairote Sattayatham)

Vice Rector for Academic Affairs

_____

(Assoc. Prof. Dr. Vorapot Khompis)

Dean of Institute of Engineering

ภาคภูมิ พูนประโคน : การทดสอบผลกระทบของความเค้นหลักกลางต่อค่ากำลังดึงของหิน (EXPERIMENTAL ASSESSMENT OF EFFECT OF INTERMEDIATE PRINCIPAL STRESSES ON ROCK TENSILE STRENGTH). อาจารย์ที่ปรึกษา : รองศาสตราจารย์ ดร.กิตติเทพ เฟื่องขจร, 76 หน้า

วัตถุประสงค์ของงานวิจัยนี้คือเพื่อทดสอบหาผลกระทบค่าความเค้นหลักกลางต่อค่ากำลังดึงของตัวอย่างหินและเพื่อพัฒนาเกณฑ์การแตกของหินภายใต้แรงดึง กิจกรรมหลักประกอบด้วย (1) การศึกษากำลังดึงของหินที่มีผลกระทบจากความเค้นที่ขนานกับระนาบรอยแตก (2) การศึกษาคุณสมบัติความยืดหยุ่นจากตัวอย่างหินที่ใช้ในการทดสอบแรงดึงแบบบราซิลโดยใช้โครงกดทดสอบในสามแกน และ (3) การพัฒนาเกณฑ์การแตกของหินภายใต้แรงดึงในสามมิติ หินทราย 3 ชนิดได้นำมาใช้ในงานวิจัยนี้คือ หินทรายชุดภูพาน ชุดภูกระดึง และชุดพระวิหาร ในการทดสอบอย่างน้อย 20 ตัวอย่างหินสำหรับหินทรายแต่ละชนิด วิธีการทดสอบจะคล้ายกับมาตรฐานสากลโดย American Society for Testing and Materials (ASTM) ยกแว้นแต่จะจะมีการเพิ่มความเค้นในแนวแกนที่คงที่บนแผ่นตัวอย่างหิน ระหว่างการกดแบบเส้นค่าความเค้นผันแปรจาก 0, 5, 10 ถึง 15 เมกะปาสกาล คุณสมบัติเชิงยืดหยุ่นที่วัดได้ถูกนำมาช่วยในการหาค่าความเค้นที่จุดเริ่มต้นของการแตก

ผลการทดสอบแรงดึงแบบบราซิลภายใต้ค่าแรงกดในแนวแกนสามารถระบุว่า ความเค้นในแนวแกนอาจทำให้เกิดความเครียดดึงในทิศทางของ σ_1 และ σ_3 เนื่องจากผลกระทบของอัตราส่วน Poisson ค่า σ_2 สามารถทำให้เกิดความเครียดดึงที่ตั้งฉากกับแกนของตัวเองได้ ค่าความเครียดดึงเพิ่มขึ้นจากค่าต่ำสุดที่จุดกึ่งกลางของตัวอย่างหินไปถึงจุดสูงสุดที่บริเวณใกล้ผิวของตัวอย่างหิน ซึ่งจุดนี้ตัวอย่างหินสามารถขยายตัวออกได้อย่างอิสระ ค่าความเครียดเหล่านี้จะช่วยให้ตัวอย่างหินเกิดการแตกแบบแยกกันง่ายขึ้น เกณฑ์ของ Coulomb และ Modified Wiebols and Cook ที่พัฒนาจากผลการทดสอบพื้นฐานได้นำมาใช้ในงานวิจัยนี้ โดยแสดงค่าความแข็งของหินในรูปของ $J_2^{1/2}$ ซึ่งอยู่ในฟังก์ชันของ J_1 เกณฑ์ของ Coulomb จะให้ค่าสูงกว่าผลการทดสอบประมาณร้อยละ 20 ในขณะที่เกณฑ์ของ Modified Wiebols and Cook ไม่สามารถอธิบายเกณฑ์การแตกของหินภายใต้แรงดึงได้

สาขาวิชา เทคโนโลยีธรณี ลายมือชื่อนักศึกษา _____

ปีการศึกษา 2552 ลายมือชื่ออาจารย์ที่ปรึกษา _____

PAKPOOM POONPRAKON : EXPERIMENTAL ASSESSMENT OF EFFECT OF INTERMEDIATE PRINCIPAL STRESSES ON ROCK TENSILE STRENGTH. THESIS ADVISOR : ASSOC. PROF. KITTITEP FUENKAJORN, Ph.D., PE., 76 PP.

TENSILE STRENGTH/ INTERMEDIATE PRINCIPAL STRESSES/ SANDSTONE/POISSON'S RATIO/ BRAZILAIN TENSION TEST

The objectives of this research are to determine the effect of the intermediate principal stress on the tensile strength of rock samples and to derive a failure criterion for rocks under tension. The effort involves (1) determination of the rock tensile strengths as affected by the stresses parallel to the incipient crack plane, (2) determination of the elastic parameters from the Brazilian samples using a polyaxial load frame, and (3) derivation of a three-dimensional tensile strength criterion. Three types of sandstone are used as rock samples Phu Phan, Phra Wihan and Phu Kradung sandstones. A minimum of 20 samples are tested for each rock type. The test method is similar to the standard practice specified by the American Society for Testing and Materials, except that constant axial stresses are applied on the disk surface during line loading. These stresses are varied from 0, 5, 10 to 15 MPa. The measured elastic parameters are used to assist in determining the induced stresses at the crack initiation point. The new tensile failure criterion presents the octahedral shear strength as a function of mean stress.

The results from the Brazilian tension tests under axial compression suggest that the axial stress may cause tensile strains in the directions of σ_1 and σ_3. Due to the effect of the Poisson's ratio, σ_2 can produce tensile strains in the directions normal to

its axis (or on the plane parallel to σ_1 and σ_3). These tensile strains increase from the minimum on the mid-section plane to the maximum on the specimen surfaces where the rock can freely dilate. These tensile strains cause splitting tensile fractures of the rock specimen. The Coulomb and modified Wiebols and Cook failure criteria derived from the characterization test results predict the sandstone strengths in term of $J_2^{1/2}$ as a function of J_1. The Coulomb criterion over-estimate the second order of the stress invariant at failure by about 20% while the modified Wiebols and Cook criterion fails to describe the rock tensile strengths.

School of Geotechnology Student's Signature_____

Academic Year 2009 Advisor's Signature_____

ACKNOWLEDGMENTS

I wish to acknowledge the funding support of Suranaree University of Technology (SUT).

I would like to express my sincere thanks to Assoc. Prof. Dr. Kittitep Fuenkajorn, thesis advisor, who gave a critical review and constant encouragement throughout the course of this research. Further appreciation is extended to Asst. Prof. Thara Lekuthai : chairman, school of Geotechnology and Dr. Prachya Tepnarong, School of Geotechnology, Suranaree University of Technology who are member of my examination committee. Grateful thanks are given to all staffs of Geomechanics Research Unit, Institute of Engineering who supported I work.

Finally, I most gratefully acknowledge my parents and friends for all their supported throughout the period of this research.

Pakpoom Poonprakon

TABLE OF CONTENTS

Page

TABLE OF CONTENTS (Continued)

Page

TABLE OF CONTENTS (Continued)

Page

LIST OF TABLES

Table **Page**

LIST OF FIGURES

Figure **Page**

LIST OF FIGURES (Continued)

Figure **Page**

LIST OF FIGURES (Continued)

Figure **Page**

LIST OF SYMBOLS AND ABBREVIATIONS

C_0	=	Uniaxial compressive strength
D	=	Disk diameter
E	=	Elastic modulus
E_n	=	Elastic modulus in the direction normal to bedding plane
E_p	=	Elastic modulus in the direction parallel to bedding plane
$J_2^{1/2}$	=	The second order of stress invariant
J_1	=	The first order of stress invariant
L	=	Disk thickness
L/D	=	Length-to-Diameter ratio
P_f	=	Failure load
S_o	=	Cohesion
ϕ	=	Friction angle
ν	=	Poisson's ratio
ν_n	=	Poisson's ratio in the direction normal to bedding plane
ν_p	=	Poisson's ratio in the direction parallel to bedding plane
σ_1	=	Maximum principal stress
σ_2	=	Intermediate principal stress
σ_3	=	Minimum principal stress
σ_B	=	Brazilian tensile stress
σ_m	=	Mean stress
σ_n	=	Normal stress

LIST OF SYMBOLS AND ABBREVIATIONS (Continued)

σ_x	=	Horizontal stress
σ_y	=	Vertical stress
σ_z	=	Axial stress
ε_x	=	Horizontal strain
ε_y	=	Vertical strain
τ	=	Shear stress
τ_{oct}	=	Octahedral shear stress

CHAPTER I

INTRODUCTION

1.1 Background of problems and significance of the study

The tensile strength of rock is one of the important parameters for the design of maximum roof span for underground mines and tunnels. The roof beam tensile strength, in many cases, dictates the extraction ratio of the ore and the size of the haulage equipments, and hence affects the economic values of the mine. The Brazilian tension test has long been used to determine the tensile strength from circular disks of rock by applying a line load along the disk diameter until failure (Jaeger and Cook, 1979). Even though this test method is widely applied and accepted, and results are incorporated into several strength criteria, a question remains on whether they can truly represent the rock tensile strength under in-situ stress states. The sample center, where the tensile crack is initiated, is subjected to biaxial plane stress condition, with the compressive stress in vertical, tensile stress in horizontal, and no stress along the sample axis. Under in-situ condition however, the roof beam is normally subjected to triaxial stress states. The influence of the stress parallel to the incipient crack plane, as normally occurred in the mine roof, has never been studied or quantitatively assessed. This is primarily because a special loading device is required to apply a constant normal stress parallel to the sample axis while the line load is applied.

1.2 Research objectives

The objectives of this research are to determine the effect of the intermediate principal stress on the Brazilian tensile strength of rock sample and to derive a new failure criterion for rocks under tension. The effort involves (1) determination of the rock tensile strengths as affected by the stresses parallel to the incipient crack plane, (2) determination of the elastic parameters from the Brazilian samples using a polyaxial load frame, and (3) derivation of a three-dimensional tensile strength criterion. Three types of sandstone will be used as rock. The test method is similar to the standard practice specified by the American Society for Testing and Materials, except that constant axial stresses will be applied on the disk surface during line loading. The measured elastic parameters, especially Poisson's ratio, are used to assist in determining the induced stresses at the crack initiation point. The new tensile failure criterion presents the octahedral shear strength as a function of mean stress. Empirical constants are incorporated into the new criterion, if needed. The research findings can improve an understanding of the tensile failure of intact rocks under a variety of stress states. The proposed failure criterion is useful in correlating the rock tensile strength obtained from the laboratory test samples with those under a more complex stress condition in the field.

1.3 Research methodology

The research methodology (Figure 1.1) comprises 5 steps; literature review, sample collection and preparation, laboratory testing, development of mathematical relations and tensile strength criterion, and discussions and conclusions.

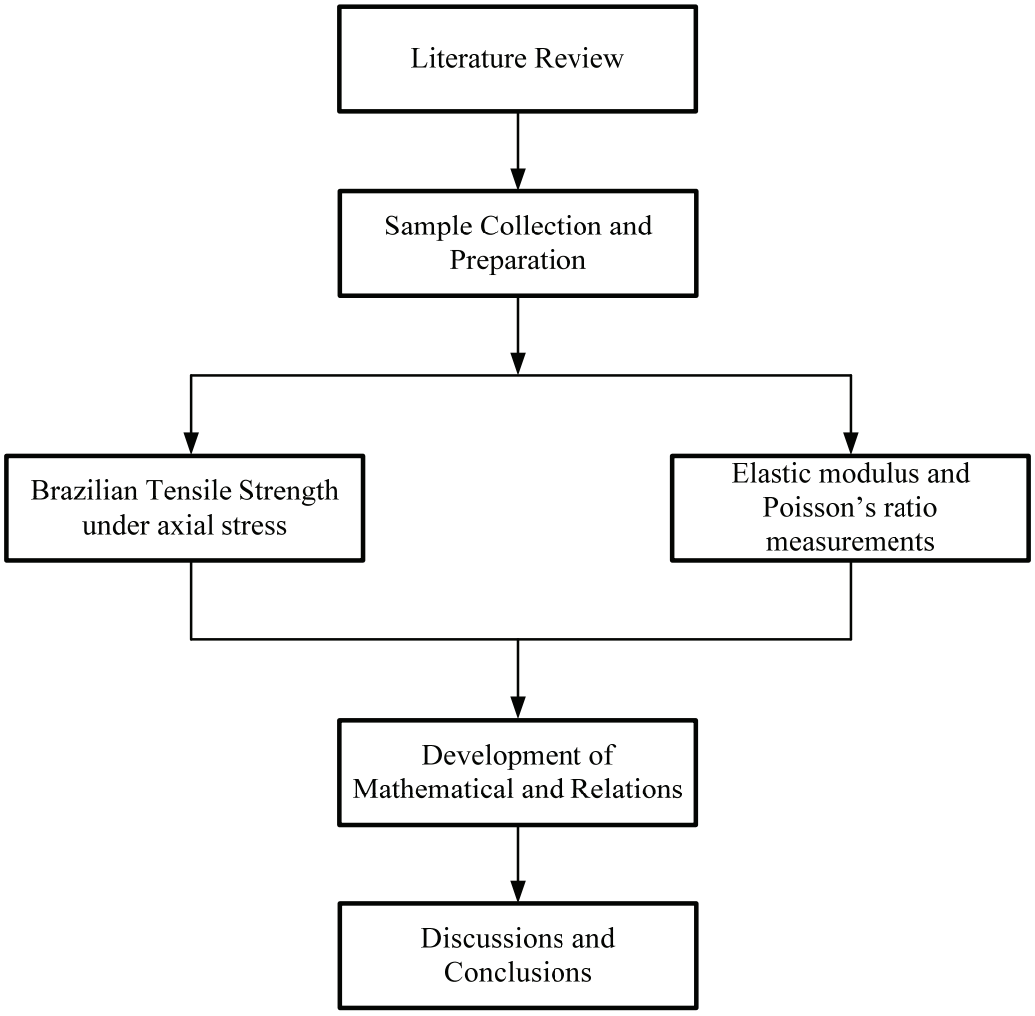

Figure 1.1 Research Methodologies

1.3.1 Literature review

Literature review is carried out to study the previous research on tensile strength test, tensile elastic modulus and tensile strength of rock. The sources of information are from text books, journals, technical reports and conference papers. A summary of the literature review is given in the thesis.

1.3.2 Sample collection and preparation

Sandstone samples are collected from the site. A minimum of 3 sandstone types are collected. Sample preparation is carried out in the laboratory at the Suranaree University of Technology. Samples prepared for Brazilian tension test have 5 cm in diameter and 2.5 cm in thickness.

1.3.3 Laboratory Testing

The laboratory testing is divided into two test series: Brazilian tension test under various axial stresses and measurements of elastic modulus and Poisson's ratio of Brazilian sample. Both tests are performed on the three rock types.

1.3.4 Brazilian tension test under various axial stresses

The Brazilian tensions under various axial stresses have been performed to determine the effects of the intermediate principal stress on the rock tensile strength. The specimen is placed in polyaxial load frame which is used to apply axial stresses to the rock. The axial stresses vary from 0 to 15 MPa. Axial load will be applied a line load is applied along the disk diameter until failure.

1.3.5 Measurements of Elastic Parameters from Brazilian samples

Set of strain gages are installed at the center of Brazilian sample to measure the deformation along and across the loading diameter. The results are used to calculate elastic modulus and Poisson's ratio of the rock.

1.3.6 Development of Mathematical Relations

Results from laboratory measurements in terms of intermediate principal stresses and the tensile strength of rock are used to formulate mathematical relations. Intermediate principal stresses and the applied stresses can be incorporated to the equation, and derive a new failure criterion for rocks under tension.

1.3.7 Thesis writing and presentation

All research activities, methods, and results are documented and complied in the thesis.

1.4 Scope and limitations of the study

Laboratory experiments are conducted on specimens from three types of sandstone, including Phu Kra-dueng, Pra Wihan, and Phu Phan formations. Testing is made under axial stress ranging from 0 to 15 MPa and up to 20 samples are tested for each rock type, with a nominal diameter of 5 cm and thickness of 2.5 cm. X-ray diffraction analysis is performed to determine the mineral compositions of the tested rocks. All tests are conducted under ambient temperature and made under dry condition.

1.5 Thesis contents

This first chapter introduces the thesis by briefly describing the rationale and background and identifying the research objectives. The third section describes research methodology. The fourth section identifies the scope and limitations. The fifth section gives a chapter by chapter overview of the contents of this thesis.

The second chapter summarizes results of the literature review. Chapter three describes samples preparation. The methods and results of the laboratory experiment are described in chapter four. Chapter five describes strength criteria. Chapter six provides the conclusion and recommendations for future research studies.

CHAPTER II

LITERATURE REVIEW

2.1 Introduction

Relevant topics and previous research results are reviewed to improve an understanding of tensile strength criterion. These include classification of tensile strength test, tensile elastic modulus and tensile strength of rock.

Specifications for the Brazilian tensile strength test have been established by American Society for Testing and Materials (ASTM D3967) and a suggested approach is provided by ISRM (Brown, 1981).

The Brazilian tensile strength (σ_B) can be calculated using the equation (Jaeger and Cook, 1979):

$$\sigma_B = \frac{2P}{\pi DL} \tag{2.1}$$

where P is the failure load, D is the disk diameter, and L is the disk thickness.

Hondros (1959) has described a method for determining Young's modulus and Poisson's ratio from strain measurement at the center of the cylinder. This method assumes that these properties are the same in tension and compression, which is not true for most rock, but may be adequate for determining these values at low stresses. The Young's modulus and Poisson's ratio can be calculated by;

$$E = 8W / \pi R(3\varepsilon_y+\varepsilon_x) \tag{2.2}$$

$$\nu = (3\varepsilon_x+\varepsilon_y) / (3\varepsilon_y+\varepsilon_x) \quad (2.3)$$

where $W = 2P\alpha R$, P is the uniform pressure over the 2α, R is the radius of the specimen and ε_x and ε_y are the strain along and normal to the load diameter at the center of the cylinder.

Claesson and Bohloli (2002) state that the tensile strength of rock is among the most important parameters influencing rock deformability, rock crushing and blasting results. To calculate the tensile strength from the indirect tensile (Brazilian) test, one must know the principal tensile stress, in particular at the rock disc center, where a crack initiates. This stress can be assessed by an analytical solution. A study of this solution for anisotropic (transversely isotropic) rock is presented. The solution is given explicitly. The key expansion coefficients are obtained from a complex-valued 2×2 matrix equation. The convergence of the solution is greatly improved by a new procedure. It is shown that the dimensionless stress field depends only on two intrinsic parameters, E'/E and b: The stress at the center of the disc is given in charts as a function of these parameters (and the angle φ_b between the direction of applied force and the plane of transverse isotropy). Furthermore, a new, reasonably accurate, approximate formula for the principal tension at the disc center, (0,0) is derived from the analytical solution:

$$\sigma_{pc}(0,0) \cong \frac{P}{\pi RL}\left[\left(\sqrt[4]{E/E'}\right)^{\cos 2\varphi_b} - \frac{\cos(4\varphi_b)}{4}(b-1)\right] \quad (2.4)$$

$$b = \frac{\sqrt{EE'}}{2}\left(\frac{1}{G'} - \frac{2\nu\nu}{E'}\right) \quad (2.5)$$

The elastic parameters of rock in two perpendicular directions were measured in the laboratory. The result of the stress analysis was applied in calculating the indirect tensile strength of gneiss, which has a well-defined foliation plane (transversely isotropic). When the results were compared with the tensile strength of rock obtained by using a conventional formula that assumes isotropic material, there was a significant difference. Moreover, good agreement was observed for the tensile strength calculated from the stress charts and the proposed formula, when compared with other published stress charts.

Haimson (2006) studies the effect of the intermediate principal stress (σ_2) on brittle fracture of rocks, and on their strength criteria. Testing equipment emulating Mogi's but considerably more compact was developed at the University of Wisconsin and used for true triaxial testing of some very strong crystalline rocks. Test results revealed three distinct compressive failure mechanisms, depending on loading mode and rock type: shear faulting resulting from extensile microcrack localization, multiple splitting along the σ_1 axis, and nondilatant shear failure. The true triaxial strength criterion for the KTB amphibolite derived from such tests was used in conjunction with logged breakout dimensions to estimate the maximum horizontal in situ stress in the KTB ultra deep scientific hole.

Liao et al. (1997) have studied the tensile behavior of a transversely isotropic rock by a series of direct tensile tests on cylindrical argillite specimens. To study the deformability of argillite under tension, two components of an electrically resistant type of strain gage with a parallel arrangement or a semiconductor strain gage are adopted for measuring the small transverse strain observed on specimens during testing. The curves of axial stress and axial strain and average volumetric strain are

presented for argillite specimens with differently inclined angles of foliation. Experimental results indicate that the stress-strain behavior depends on the foliation inclination of specimens with respect to the loading direction. The five elastic constants of argillite are calculated by measuring two cylindrical specimens. Based on theoretical analysis results, the range of the foliation inclination of the specimens tested is investigated for feasibility obtaining the five elastic moduli. A dipping angle of the foliations (φ) of 30-60° with respect to the plane normal to the loading direction is recommended. The final failure modes of the specimens are investigated in detail. A sawtoothed failure plane occurs for the specimens with a high inclination of foliation with respect to the plane perpendicular to the loading direction. On the other hand, a smooth plane occurs along the foliation for specimens with low inclination of foliation with respect to the plane normal to the loading direction. A conceptual failure criterion of tensile strength is proposed for specimens with a high inclination of foliation.

Singh et al. (1998) state that the Mohr-Coulomb criterion needs to be modified for highly anisotropic rock material and jointed rock masses. Taking σ_2 into account, a new strength criterion is suggested because both σ_2 and σ_3 would contribute to the normal stress on the existing plane of weakness. This criterion explains the enhancement of strength (σ_2 - σ_3) in the underground openings because σ_3 along the tunnel axis are not relaxed significantly. Another cause of strength enhancement is less reduction in the mass modulus in tunnels due to constrained dilatancy. Empirical correlations obtained from data from block shear tests and uniaxial jacking tests have been suggested to estimate new strength parameters. A correlation for the tensile strength of the rock mass is presented. Finally, Hoek and Brown theory is extended to

account for a σ_2. A common strength criterion for both supported underground openings and rock slopes is suggested.

Tepnarong (2001) states that a modified point load (MPL) testing technique can be used to correlate the results with the uniaxial compressive strength (UCS) and tensile strength of intact rock. The primary objective is to develop an inexpensive and reliable rock testing method for use in the field and in the laboratory. The test apparatus is similar to that of the conventional point load (CPL), except that the loading points are cut flat to have a circular cross-section area instead of using a half-spherical shape. To derive a new solution, finite element analyses and laboratory experiments have been carried out. The simulation results suggest that the applied stress required failing the MPL specimen in creases logarithmically as the specimen thickness or diameter increases. The maximum tensile stress occurs directly below the loading area with a distance approximately equal to the loading diameter. The MPL test, CPL test, UCS test, and Brazilian tension test have been performed on Saraburi mable under variety of sizes and shapes. The UCS test results indicate that the strengths decrease with increasing length-to-diameter ratio. The test results can be postulated that the MPL strength can be correlated with the compressive strength when the MPL specimens are relatively thin, and should de indicator of the tensile strength when the specimens are significantly larger than the diameter of the loading points. Predictive capability of the MPL and CPL techniques has been assessed and compared. Extrapolation of the test results suggest that the MPL results predict the UCS of the rock specimens better than does the CPL testing. The tensile strength predicted by MPL also agrees reasonably well with the Brazilian tensile strength of the rock.

Wang et al. (2009) studies the Flattened Brazilian Disc (FBD) specimens which were impacted diametrically by a pulse shaping split Hopkinson pressure bar to measure dynamic tensile strength of a brittle rock. With application of strain gauge technique, the stress waves traveling through the incident bar, the transmission bar as well as the FBD specimen were recorded and analyzed. The loading history was determined based on the one-dimensional stress wave theory. The dynamic equilibrium condition in the specimen was approximately satisfied, this claim was supported by the numerical simulation of dynamic stress evolution in the specimen, with the conclusion that a short time after impact the pattern of dynamic stress distribution in the specimen was symmetric and similar to that of the counterpart static loading. The validity of the test was further verified experimentally, as the waveforms acting on the two flat ends of the FBD specimen, respectively, were of nearly the same shape, and the rupture modes of the specimens were generally such that crack first initiated at the center of the disc and subsequently propagated along the loading diameter, whereas crush zones were implied to form lastly near the two flat ends of the broken specimen. The dynamic tensile strength of marble was measured at the critical point when the tensile strain wave.

Lanaro et al. (2009) study the influence of initiated cracks on the stress distribution within rock samples subjected to indirect tensile loading by traditional Brazilian testing. The numerical analyses show that the stress distribution inside the models is only marginally affected by the friction between the loading platens and the sample. On the other hand, the initiation and propagation of cracks produce a stress field that is very different from that assumed by considering the rock material as continuous, homogeneous, isotropic and elastic. In the models, stress concentrations

at the bridges between the cracks were found to reach tensile stresses much higher than the direct tensile strength of the intact rock input in the numerical models. This was due to the development of large stress gradients between the cracks. The analysis of the deformation along the sample diameter perpendicular to the loading direction might enable one to determine the direct tensile strength of the rock. In fact, when the tensile strength is reached, initiation of cracks in the sample induces a sudden increase of the rate of the diametric strains. The direct tensile strength is therefore indicated by the point where the stress–strain curves in the direction perpendicular to the loading diameter depart from linearity.

Jianhong et al. (2008) state that the tensile elastic modulus E_t of a rock is different from the compressive elastic modulus E_c, due to inhomogeneity and microcracks. There is no convenient method to obtain E_t except using direct tension tests. However, the direct tension test for rock materials is difficult to perform, because of stress concentrations, and the difficulty of preparing specimens. We have developed a new method to determine E_t of rock materials easily and conveniently. Two strain gauges are pasted at the center part of a Brazilian disc's two side faces along the direction perpendicular to the line load to record tensile strain, and a force sensor is used to record the force applied, then the stress–strain curve can be obtained, finally the E_t can be calculated according to those related formulas which are derived on the basis of elasticity theory. There experimental results for marble, sandstone, limestone and granite indicate that E_t is less than E_c, and their ratio is generally between 0.6 and 0.9.

Wang et al. (2003) studies the flattened Brazilian disc specimen which is proposed for determination of the elastic modulus E, tensile strength σ_t and opening

mode fracture toughness K_{IC} for brittle rocks in just one test. This paper is concerned with the theoretical analysis as well as analytical and numerical results for the formulas. According to the results of stress analysis and Griffith's strength criteria, in order to guarantee crack initiation at the centre of the specimen, which is considered to be crucial for the test validity, the loading angle corresponding to the flat end width must be greater than a critical value ($2\alpha \geq 20°$). The analysis shows that, based on the recorded complete load-displacement curve of the specimen (the curve should include the 'fluctuation' section after the maximum load), E can be determined by the slope of the section before the maximum load, σ_t by the maximum load, and K_{IC} by the local minimum load immediately subsequent to the maximum load. The relevant formulas for the calculation of E, σ_t, K_{IC} are obtained, and the key coefficients in these formulas are calibrated by finite-element analysis. In addition, some approximate closed-form formulas based on elasticity are provided, and their accuracy is shown to be adequate by comparison with the finite-element results.

Chen et al. (1998) determine of the deformability, tensile strength and fracturing of anisotropic rocks by diametral compression (Brazilian test) of discs of rock. It presents a combination of analytical and experimental methods for determining in the laboratory the elastic constants and the indirect (Brazilian) tensile strength of transversely isotropic rocks, i.e. rocks with one dominant direction of planar anisotropy. A computer program based on the complex variable function method and the generalized reduced gradient method was developed to determine the elastic constants of idealized linearly elastic, homogeneous, transversely isotropic media from the strains measured at the center of discs subjected to diametral loading. The complex variable function method was also used to construct charts for

determining the indirect tensile strength of anisotropic media from the failure loads measured during diarnetral loading. Brazilian tests were conducted on four types of bedded sandstones assumed to be transversely isotropic. Based on strain measurements obtained with 45° strain gage rosettes glued at the center of the discs, the five independent elastic constants of the tested rocks could be determined. The elastic constants determined with the Brazilian tests were compared with those obtained from conventional uniaxial compression tests. The indirect (Brazilian) tensile strength of the tested sandstones was found to depend on the angle between the apparent planes of rock anisotropy and the direction of diametral loading.

Diederichs and Kaiser (1999) have proposed classical assessment of instability potential in underground excavations are normally based on yield and rupture criteria for stress driven failure and on limit equilibrium analysis of structurally controlled failure. While it is true that ultimate failure and falls of ground can be an eventual consequence of stress fracturing and unfavourable structure within the rock mass, the timing of such failure is often controlled by the presence of residual tensile capacity, in the form of rock bridges separating joint segments and fractures and by the mechanisms of clamping and relaxation. Using crack and rock-bridge analogues in conjunction with an updated voussoir beam model, this paper explores the influence of residual tensile strength and boundary parallel relaxation on the failure process. The impact on support design is also examined. In underground hard rock mines with complex geometries and interacting openings, relaxation is identified as a key controlling factor in groundfall occurrence. Empirical stability assessment techniques for underground tunnels and for mining stopes are updated to account for relaxation.

Tien et al. (2006) have proposed the results of an experimental investigation of the failure mechanism, including failure process and failure modes, of transversely isotropic rock. This paper employs a rotary scanner to obtain the ‘‘unrolled’’ images of rock specimens at different stress levels during the uniaxial compressive tests. The unrolled image constitutes a circumferential surface image of the cylindrical specimen in a single picture and facilitates the study of failure processes and failure modes. Based on the experimental results, the failure of simulated transversely isotropic rock with varied orientations at different confining pressures is classified into one of two modes (a) sliding failure along the discontinuities and (b) non-sliding failure along the discontinuities. The latter can be further classified into one of the following three sub-failure modes (1) tensile fracture across the discontinuities, (2) tensile-split along the discontinuities, and (3) sliding failure across the discontinuities. The failure processes of these modes are also examined in this study. Failure criterion proposed by Tien and Kuo is found to predict accurately the strength and failure modes of simulated transversely isotropic rocks.

Cai (2007) studied the influence of the intermediate principal stress on rock fracturing and strength near excavation boundaries is studied using a FEM/DEM combined numerical tool. A loading condition of $\sigma_3 = 0$ and $\sigma_1 \neq 0$, and $\sigma_2 \neq 0$ exists at the tunnel boundary, where σ_1, σ_2, and σ_3, are the maximum, intermediate, and minimum principal stress components, respectively. The numerical study is based on sample loading testing that follows this type of boundary stress condition. It is seen from the simulation results that the generation of tunnel surface parallel fractures and microcracks is attributed to material heterogeneity and the existence of relatively high intermediate principal stress (σ_2), as well as zero to low minimum principal stress (σ_3)

confinement. A high intermediate principal stress confines the rock in such a way that microcracks and fractures can only be developed in the direction parallel to σ_1 and σ_2. Stress-induced fracturing and microcracking in this fashion can lead to onion-skin fractures, spalling, and slabbing in shallow ground near the opening and surface parallel microcracks further away from the opening, leading to anisotropic behavior of the rock. Hence, consideration of the effect of the intermediate principal stress on rock behavior should focus on the stress-induced anisotropic strength and deformation behavior of the rocks. It is also found that the intermediate principal stress has limited influence on the peak strength of the rock near the excavation boundary.

Ohokal et al. (1997) have studied the tensile test using hollow cylindrical specimen is suitable for evaluating mechanical properties of soft rock under controlled conditions of the pore water. The authors tried to adopt this test for the Tertiary tuff, and got satisfactory results as follows; 1) Typical tensile failure modes are observed in any specimens 2) According to increase the confining pressure, stress-strain curves appear nonlinear behaviors and failure strains increase 3) Tensile strengths seem to be constant regardless of confining pressure.

CHAPTER III

SAMPLE PREPARATION

3.1 Introduction

The tested sandstones are from three sources: Phu Phan, Phra Wihan and Phu Kradung formations (hereafter designated as PP, PW and PK sandstones) (Figure 3.1). These fine-grained quartz sandstones are selected primarily because of their highly uniform texture, density and strength. The main mineral compositions of three sandstones obtained from x-ray diffraction analyses are given in Table 3.1. Their average grain size is 0.1-1.0 mm. They are commonly found in the north and northeast of Thailand. Their mechanical properties and responses play a significant role in the stability of tunnels, slope embankments and dam foundations in the region.

3.2 Sample preparation and collection

Sample preparation is conducted in laboratory facility at the Suranaree University of Technology. The process includes coring and cutting (Figures 3.2 through 3.3). Preparation for the Brazilian tension test under axial stress uses disk specimens with a nominal diameter of 50 mm with a thickness-to-diameter ratio of 0.5 to comply with ASTM D 3967-95 (Figure 3.4). A total of 40 specimen are prepared for Elastic parameter measurements use the Brazilian tension disks having a nominal diameter of 100 mm with L/D ratio of 2.0 (Figure 3.5). Over 40 samples have been prepared for each rock type. The core axis is normal to the bedding planes. All specimens are oven-dried before testing.

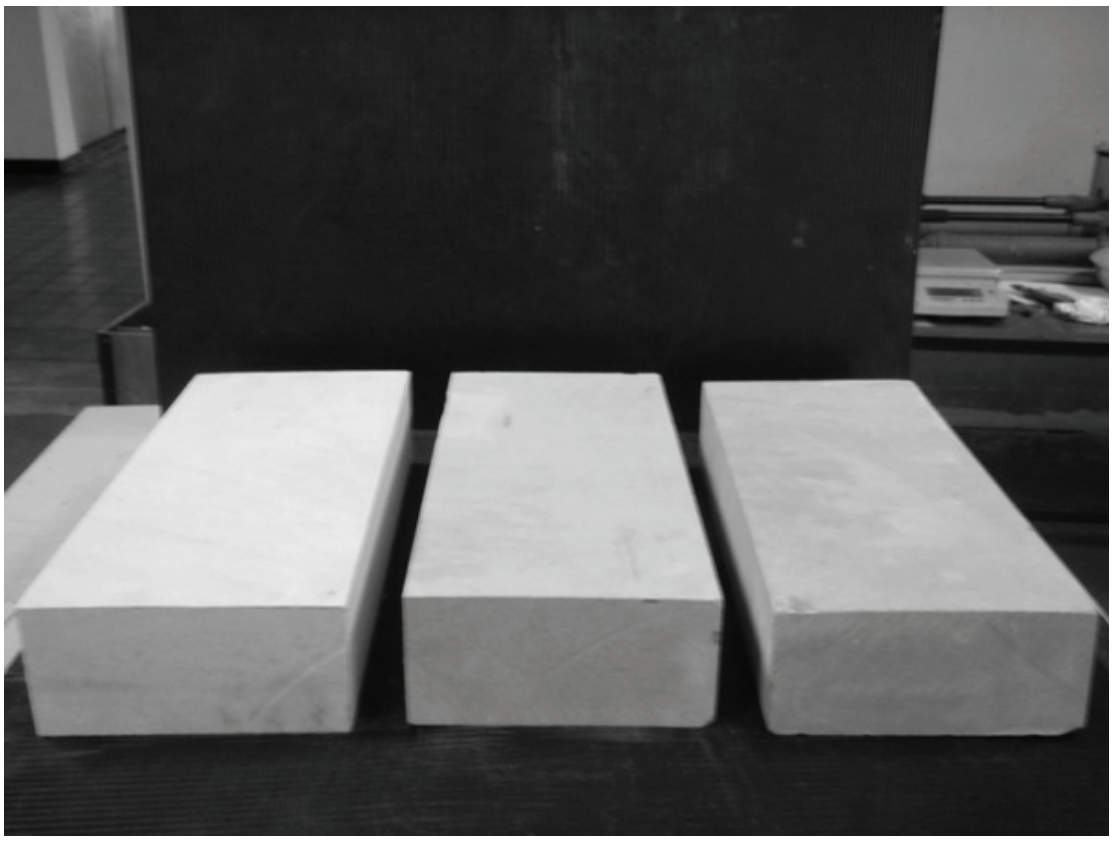

Figure 3.1 Sandstones blocks with nominal size of 10 cm x 20 cm x 40 cm are from Saraburi province.

Table 3.1 Mineral compositions of three sandstones

Rock sample	Density (g/cc)	Color	Compositions				
			Quartz (%)	Albite (%)	Kaolinite (%)	Feldspar (%)	Mica (%)
PW sandstone	2.35	white	99.47	-	0.53	-	-
PP sandstone	2.45	yellow	98.40	-	-	-	1.60
PK sandstone	2.63	green	48.80	46.10	5.10	-	-

Figure 3.2 Laboratory core drilling. The core drilling machine (model SBEL 1150) is used to drill core specimens using diamond impregnated bit with diameter of 54 mm.

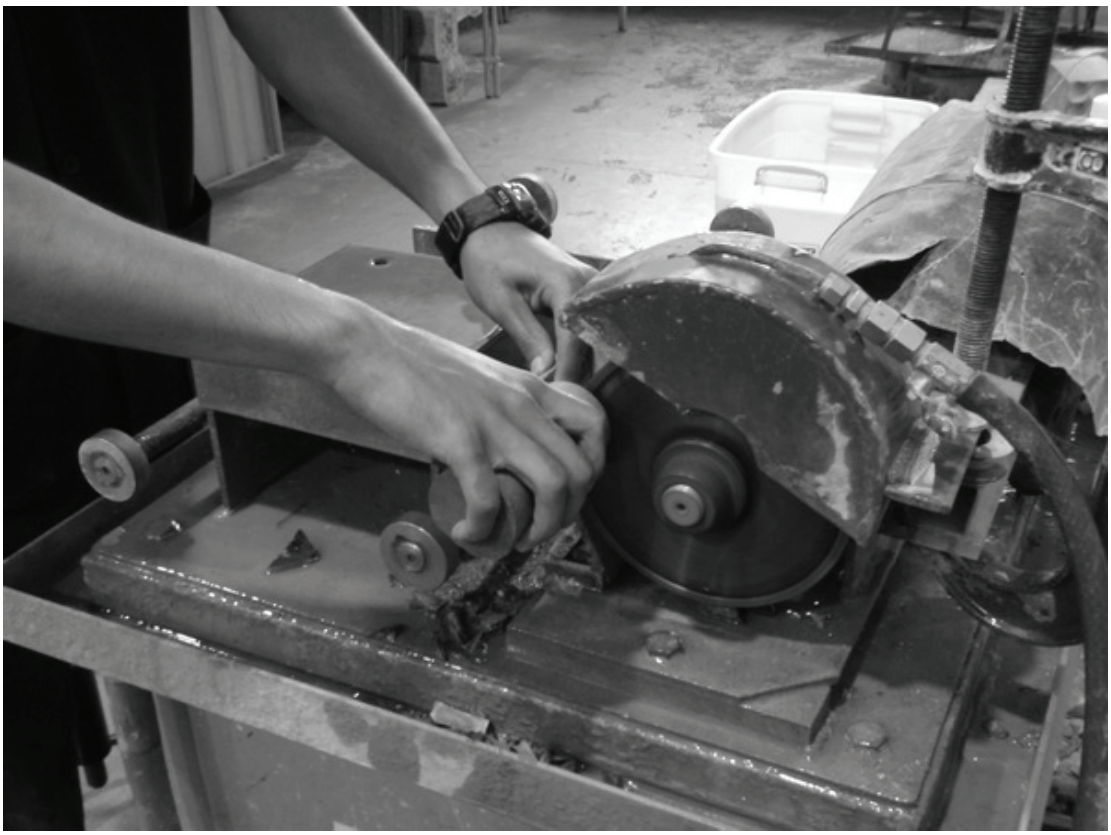

Figure 3.3 A core specimen of sandstone is cut by a cutting machine.

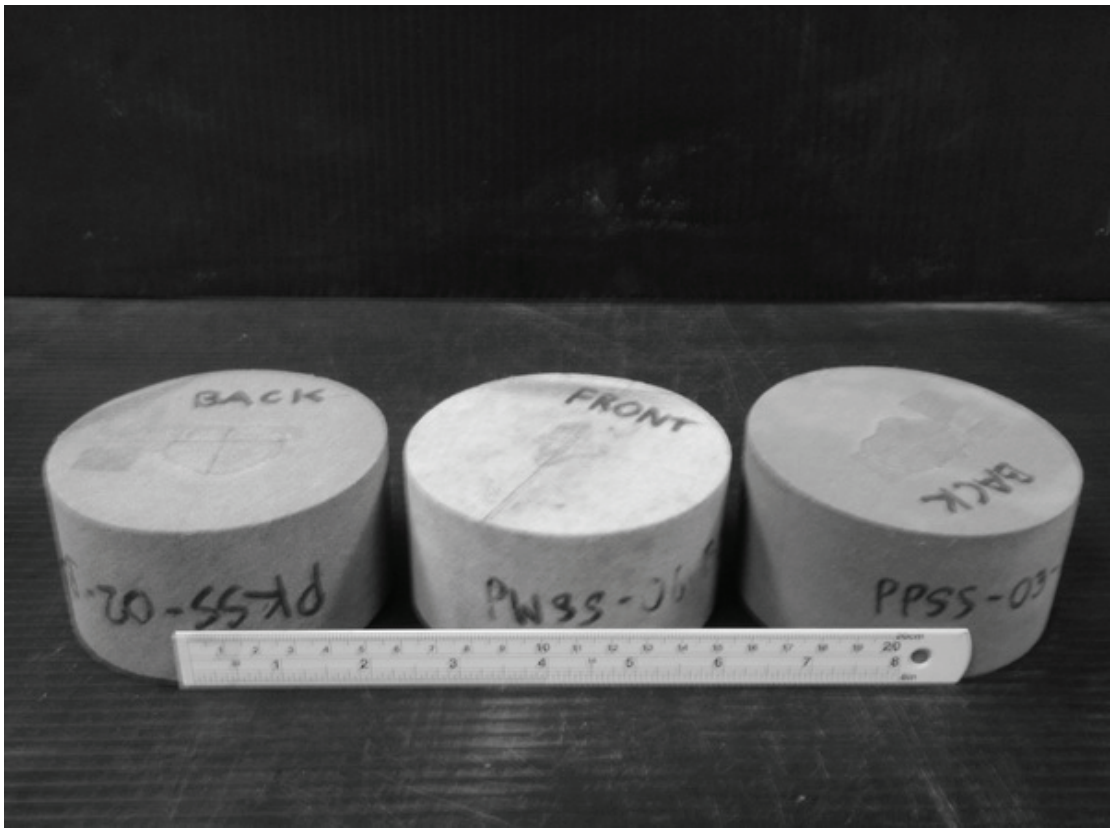

Figure 3.4 Sandstone specimens prepared for the Brazilian tension test under confinements.

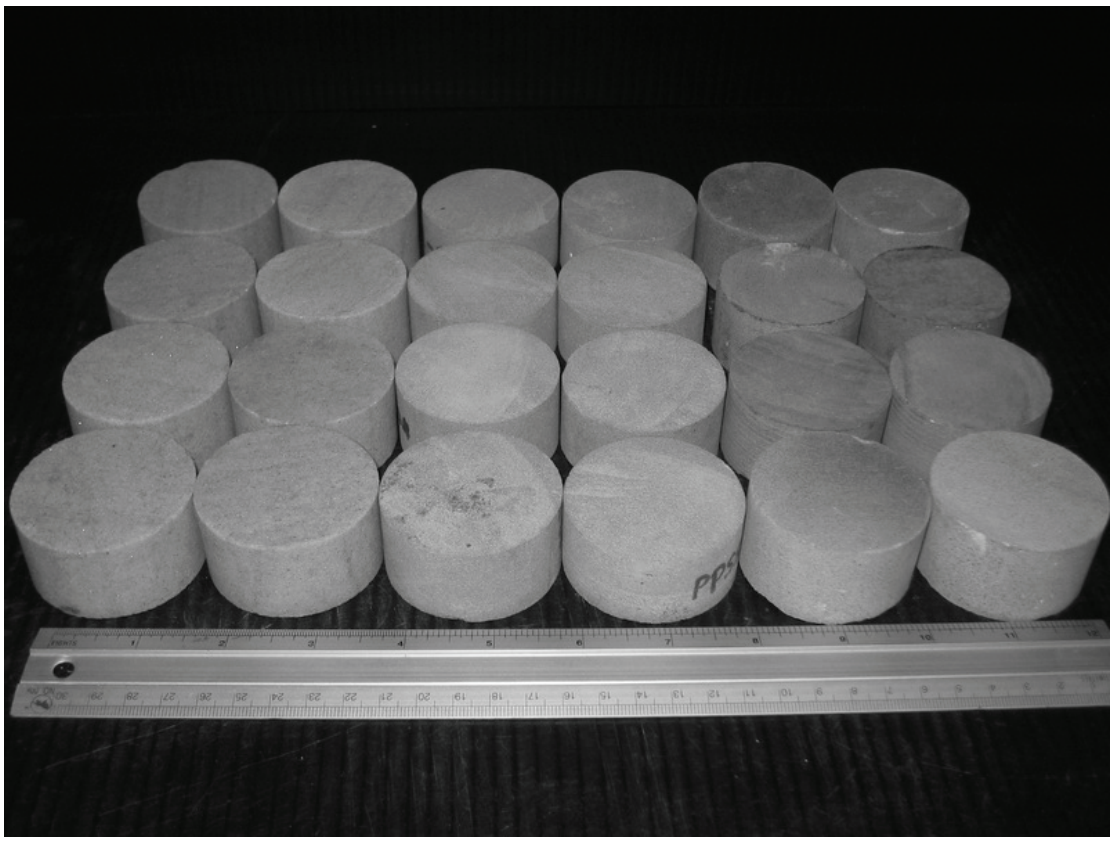

Figure 3.5 Sandstone specimens prepared for elastic parameter measurements.

CHAPTER IV

LABORATORY EXPERIMENTS

4.1 Introduction

The objectives of the laboratory experiments are to determine the effects of the intermediate principal stress on the rock tensile strength and to measure of the elastic parameters from the Brazilian tension test. This chapter describes the method and results of the laboratory experiments. It is divided into two parts; Brazilian tension tests under axial compression and measurements of elastic modulus and Poisson's ratio from the Brazilian test specimens.

4.2 Brazilian tension tests under axial compression

The Brazilian tension tests with axial compression have been performed on PP, PW and PK sandstone disks to determine the effects of the intermediate principal stresses on the rock tensile strength. The polyaxial load frame is used to apply the constant axial stresses on the disk specimen (Figures 4.1 through 4.3) while the diametral line load apply by hydraulic load cell until failure. The constant axial stress is varied from zero (Brazilian test) to as high as the rock compressive strength. The specimens are prepared to have a nominal diameter of 50 mm with a thickness-to-diameter ratio of 0.5 to comply with the ASTM D 3967-95. All specimens have the core axis normal to the bedding planes (Figure 4.4). Neoprene sheets are used to minimize the friction between the rock surface and loading platen in the axial direction.

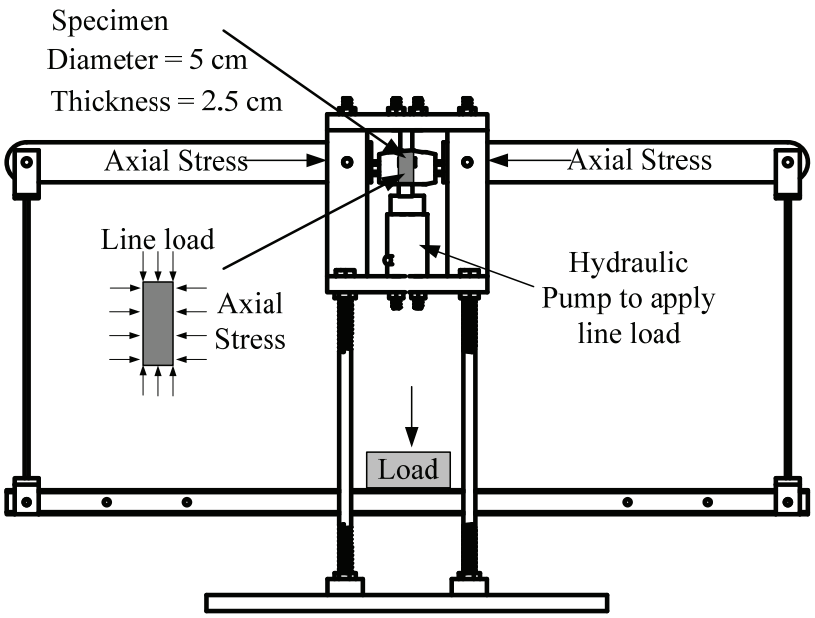

Figure 4.1 Laboratory set-up for Brazilian tensile strength test under

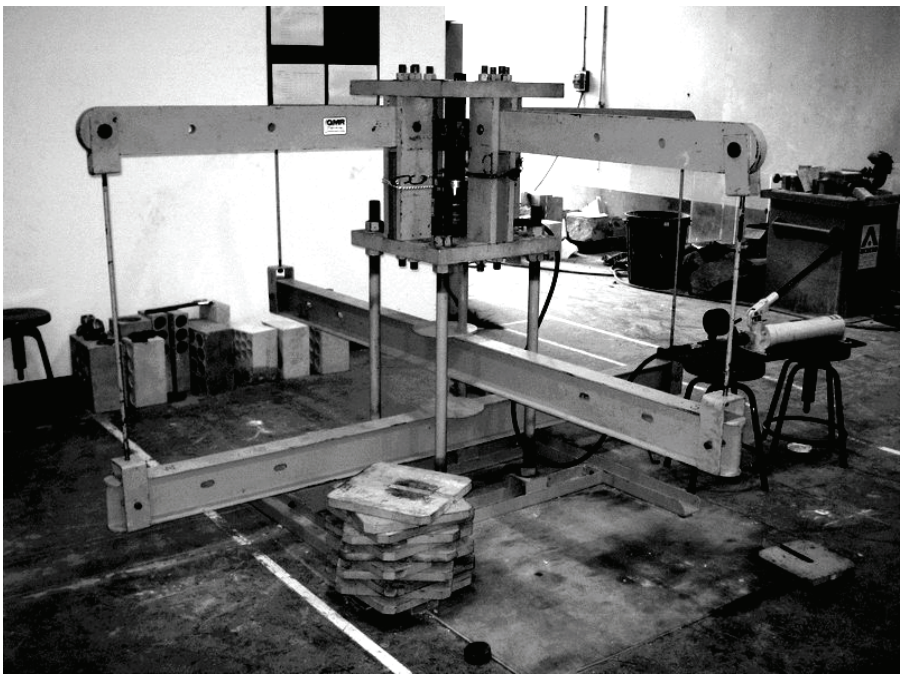

Figure 4.2 Polyaxial load frame developed for strength testing under true triaxial stress.

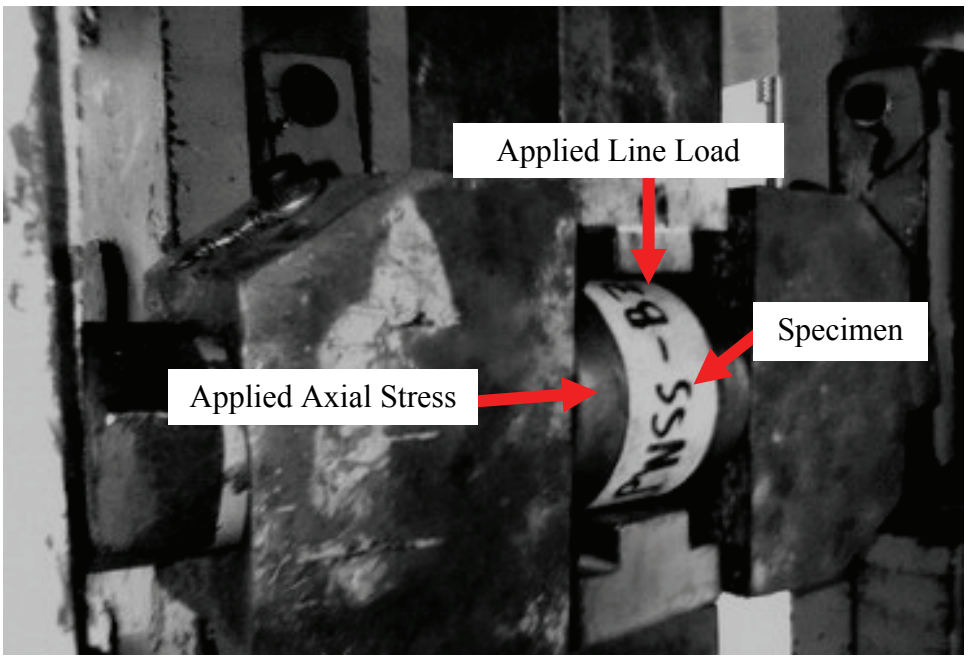

Figure 4.3 PW sandstone specimen is placed in the polyaxial load frame.

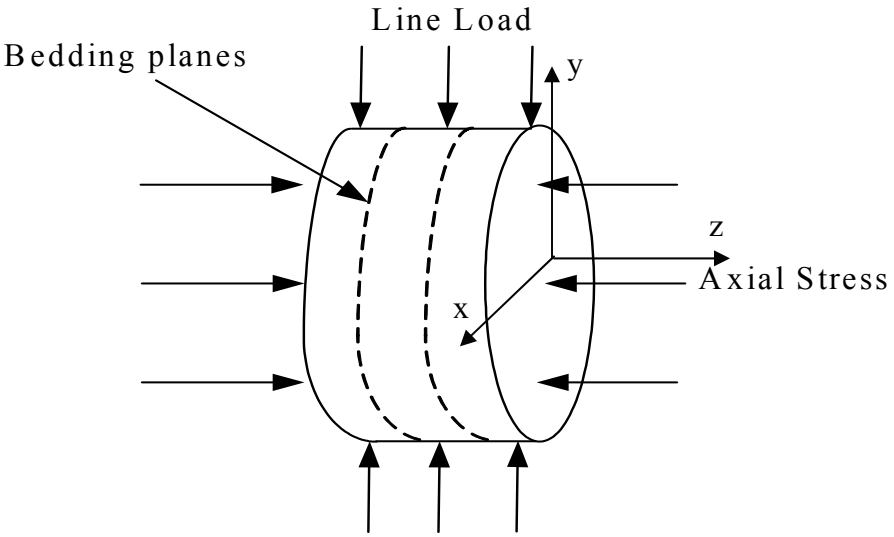

Figure 4.4 The applied stress directions with respect to the bedding planes for all specimens.

4.2.1 Test Results

The Brazilian tensile strength (σ_B) can be calculated using the equation (Jaeger and Cook, 1979):

$$\sigma_B = \frac{2P_f}{\pi DL} \tag{4.1}$$

where σ_B is the Brazilian tensile strength, P_f is the failure load, D is the disk diameter and L is the disk thickness.

The failure load linearly decreases with increasing axial stress (Figure 4.5). At $P_f = 0$ the axial stress becomes the uniaxial compressive strength of the rock. The tensile stresses (σ_x) and compressive stresses (σ_y) induced at the crack initiation point in the middle of the specimen also decrease with increasing axial stress (Figure 4.6). The stress state in the middle of the specimen at failure is determined as (Jaeger and Cook, 1997):

$$\sigma_x = \frac{2P_f}{\pi DL} \tag{4.2}$$

$$\sigma_y = 3\sigma_x \tag{4.3}$$

σ_z = Applied axial stress

At this point σ_y, σ_x and σ_z represent the principal stresses. The induced tensile stress σ_x is always the minimum principal stress. The magnitudes of the applied axial stress determine whether σ_y or σ_z is the maximum principal stress. Under low applied σ_z, σ_y

is the maximum principal stress and σ_z is the intermediate principal stress. Under high σ_z, σ_y becomes the intermediate principal stress and σ_z is the maximum principal stress. The strength results can be presented in form of τ_{oct} as a function of σ_m in Figure 4.7.

Where:

$$\sigma_m = \frac{1}{3}(\sigma_1 + \sigma_2 + \sigma_3) \tag{4.4}$$

$$\tau_{oct} = \frac{1}{3}\left\{(\sigma_1 - \sigma_2)^2 + (\sigma_2 - \sigma_3)^2 + (\sigma_3 - \sigma_1)^2\right\}^{\frac{1}{2}} \tag{4.5}$$

The figure shows the optimum mean stress corresponding to the point at which the lowest shear stress is required to fail the rock sample. These optimum mean stresses are 8, 12 and 13 MPa for PW, PK and PP sandstones, respectively.

This test series also reveal a linear transition from the Brazilian tensile strength to the uniaxial compressive strength, which can be best demonstrated by using Mohr's circles, as shown in Figures 4.8 through 4.10.

Post-failure observations show that under low σ_z a single splitting extension crack along the loading diameter is normally induced in the disk specimen. Multiple extension cracks are developed as σ_z increase. When σ_z reaches the uniaxial compressive strength of the rocks, the specimens fail without applying the diametral line load. At this point the specimens are crushed, resulting in multiple shear fractures and extension cracks (Figure 4.11).

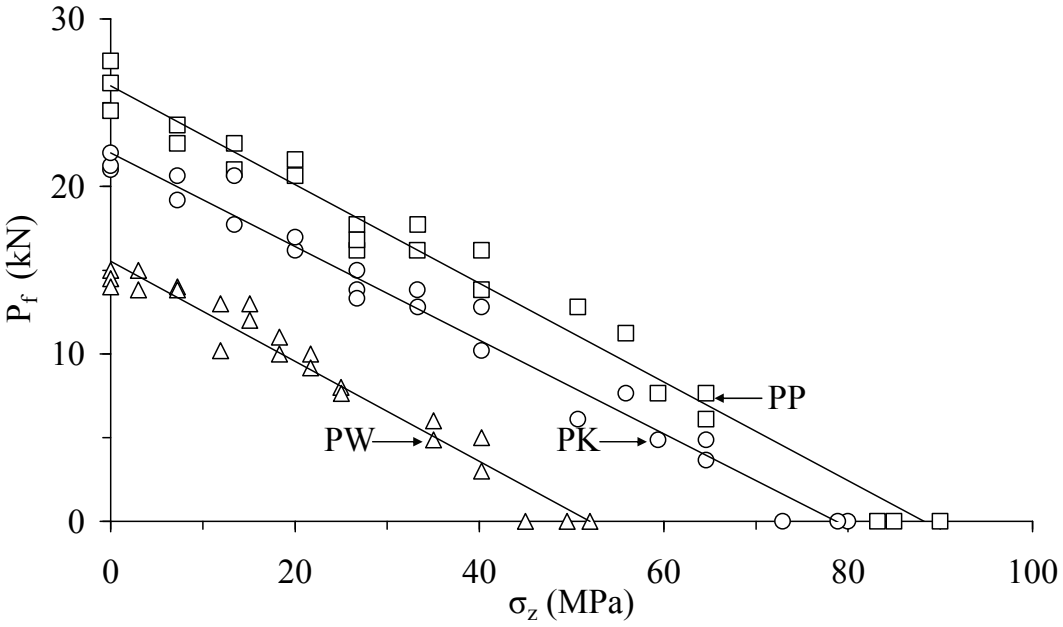

Figure 4.5 Line load at failure (P_f) as a function of applied axial stress (σ_z).

It is postulated that the axial stress produces tensile strains perpendicular to its direction due to the effect of the Poisson's ratio. At the crack initiation point this tensile strain is combined with the horizontal tensile stress that is induced by the line load. The line load at failure therefore decreases with increasing σ_z. Calculation of the σ_z-induced tensile strain for the entire specimen is however not that simple because the rock is under both tension and compression and the elastic properties under tension and compression may be different (Jaeger & Cook, 1979; Chen et al., 1998). More discussion on this issue is given in the next section.

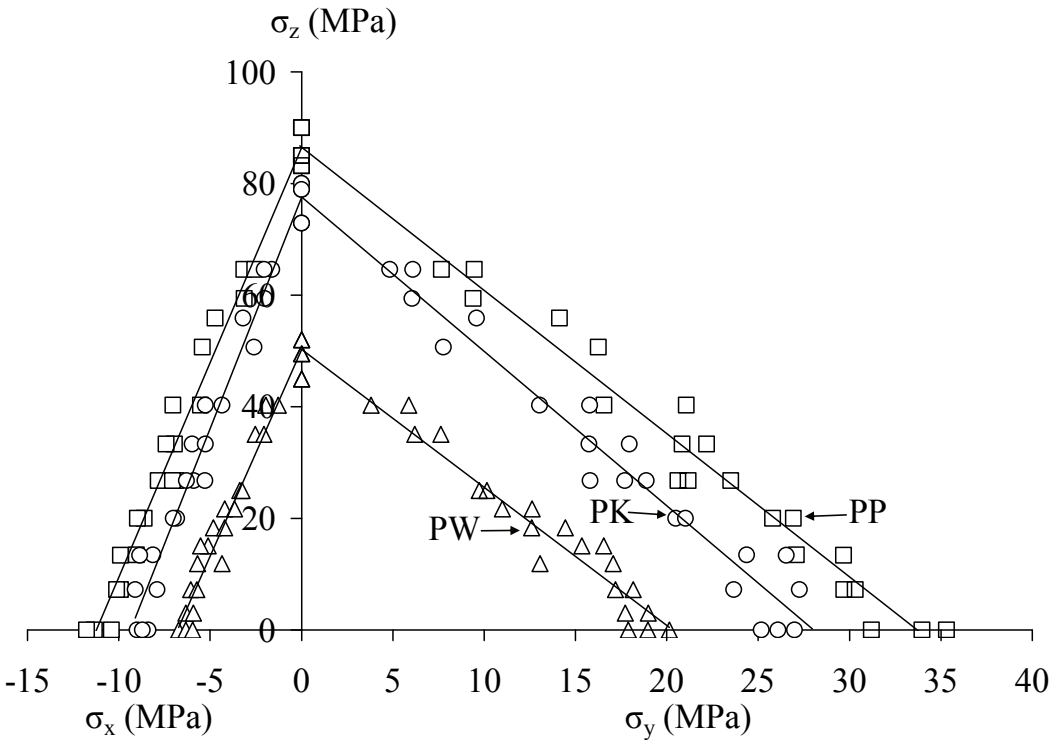

Figure 4.6 Induced compressive (σ_y) and tensile stresses (σ_x) at failure as a function of applied σ_z.

4.3 Measurements of elastic parameters from Brazilian samples

The elastic modulus and Poisson's ratio are measured under no axial stress and calculated at 30% of the rock tensile strength (PP sandstone from 0 to 30 kN, PK sandstone from 0 to 30 kN and PW sandstone from 0 to 20 kN). The specimens have a nominal diameter of 100 mm with L/D ratio of 0.5. Their core axis is normal to the bedding planes. They are measured by installing strain gages at the center of the sandstone specimen and connect with the strain-meter. The gages measure the vertical compressive strain, ε_y, (along the loading diameter) and its perpendicular horizontal tensile strain, ε_x, induced during line loading (Figures 4.12 through 4.13). Three samples have been tested for each rock type.

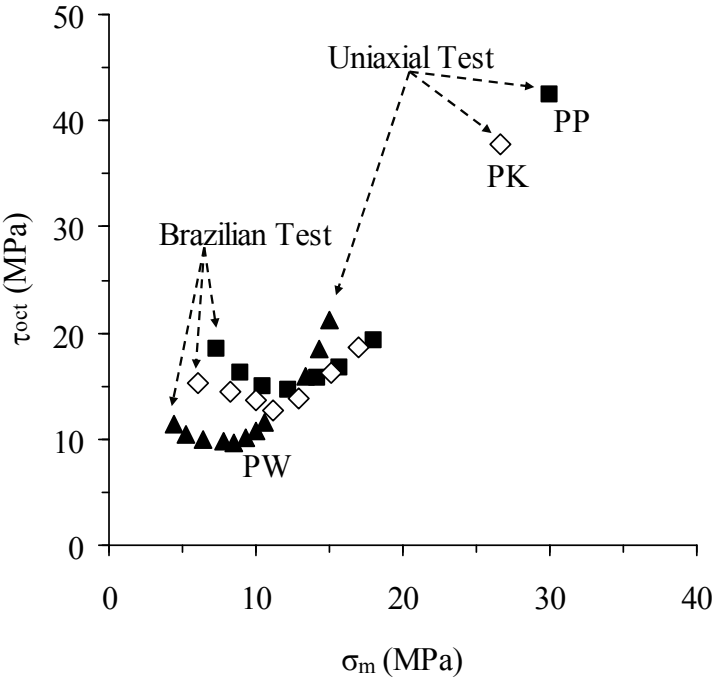

Figure 4.7 Octahedral shear stress (τ_{oct}) as a function of mean stress (σ_m) for three sandstones.

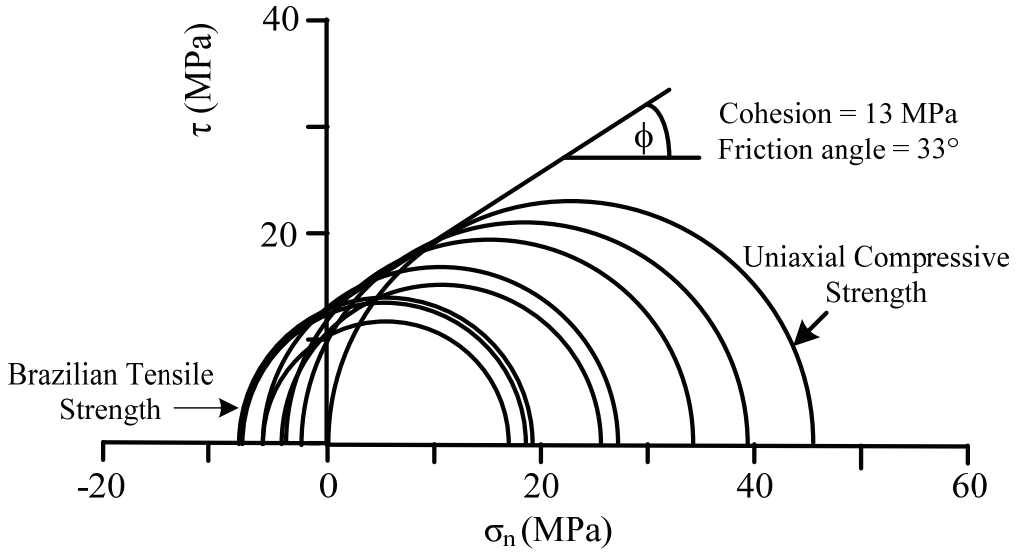

Figure 4.8 Mohr's circles from testing of PW sandstone showing transition from Brazilian tensile strength to uniaxial compressive strength.

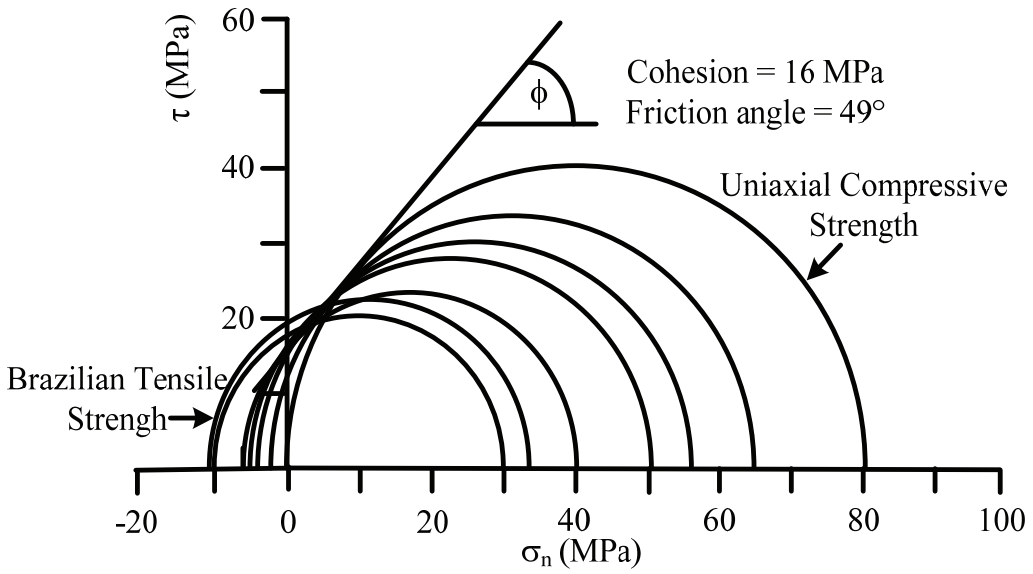

Figure 4.9 Mohr's circles from testing of PP sandstone showing transition from Brazilian tensile strength to uniaxial compressive strength.

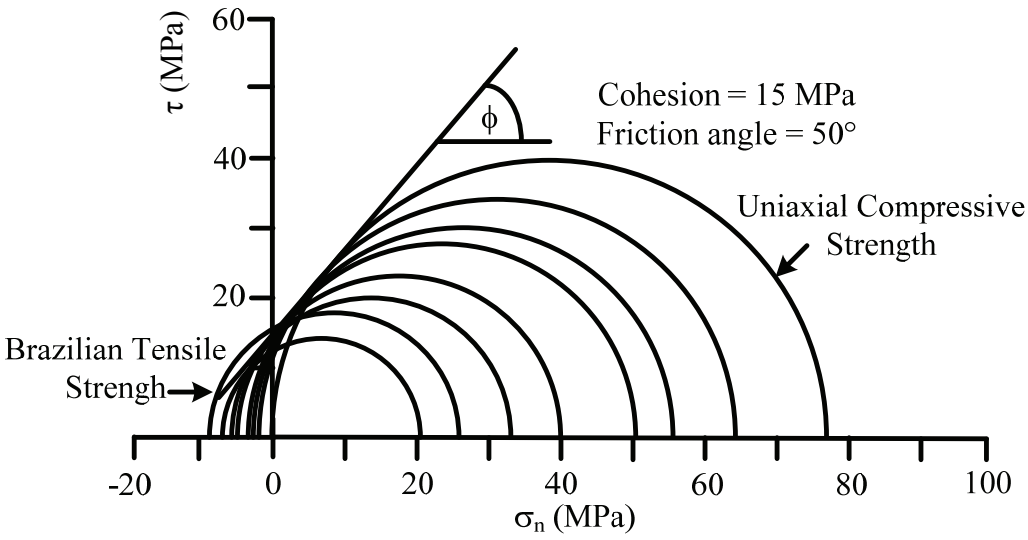

Figure 4.10 Mohr's circles from testing of PK sandstone showing transition from Brazilian tensile strength to uniaxial compressive strength.

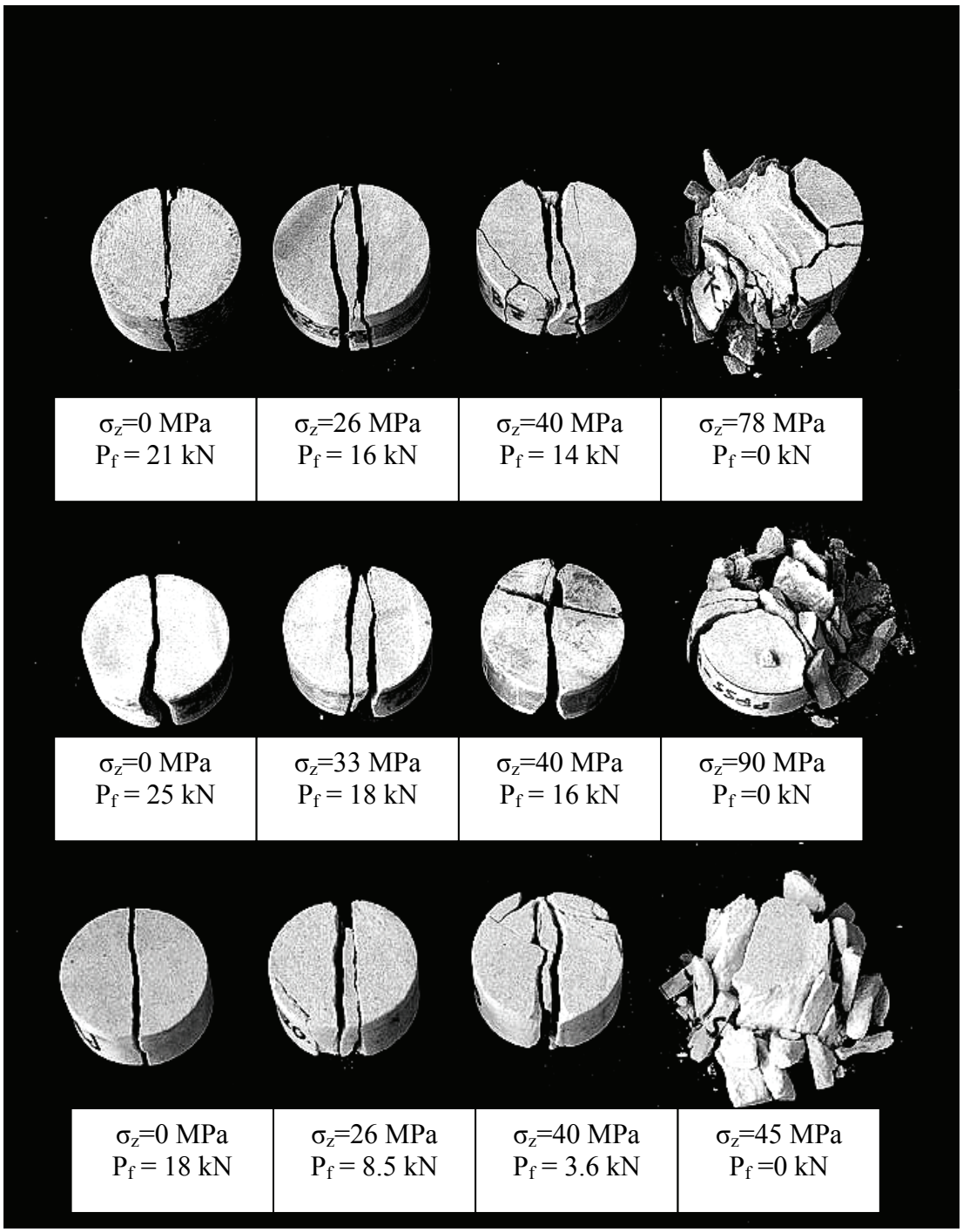

Figure 4.11 Some post- test specimens of PK sandstone (top), PP sandstone (middle) and PW sandstone (bottom).

4.3.1 Test Results

The elastic modulus (E) and Poisson's ratio (ν) can be calculated using the following equations (Hondros, 1959):

$$\nu = -\frac{3\varepsilon_x + \varepsilon_y}{3\varepsilon_y + \varepsilon_x} \tag{4.6}$$

$$E = \frac{2P(1-\nu)^2}{\pi Dt(\varepsilon_x + \nu\varepsilon_y)} \tag{4.7}$$

These equations assume that the rock is linearly elastic and isotropic and that the elastic modulus in tension is equal to that in compression.

The results of the vertical compressive strain (ε_y) and horizontal tensile strain (ε_x) measurements for PW, PK and PP sandstones are given in Figure 4.14. The E and ν above are compared with those obtained from the related polyaxial compression testing by (Walsri et al, 2009) in Table 4.1. Since all Brazilian disks are prepared to have bedding planes normal to the disk axis, only elastic modulus and Poisson's ratio parallel to the bedding (ν_p) can be measured. The discrepancy of the elastic parameters obtained from the two test types may be because the rock elastic modulus under tension is lower than that under compression and there is intrinsic variability among the tested specimens.

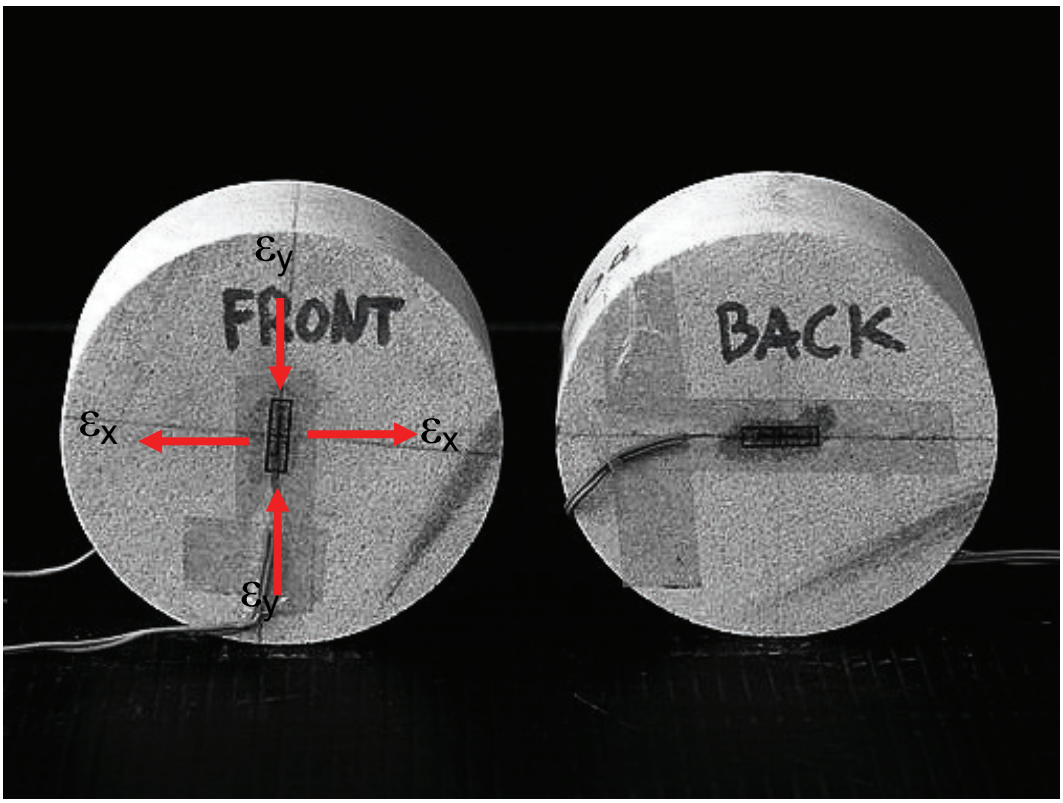

Figure 4.12 A strain gage is installed to obtain vertical compressive strain (ε_y) and horizontal tensile strain (ε_x)

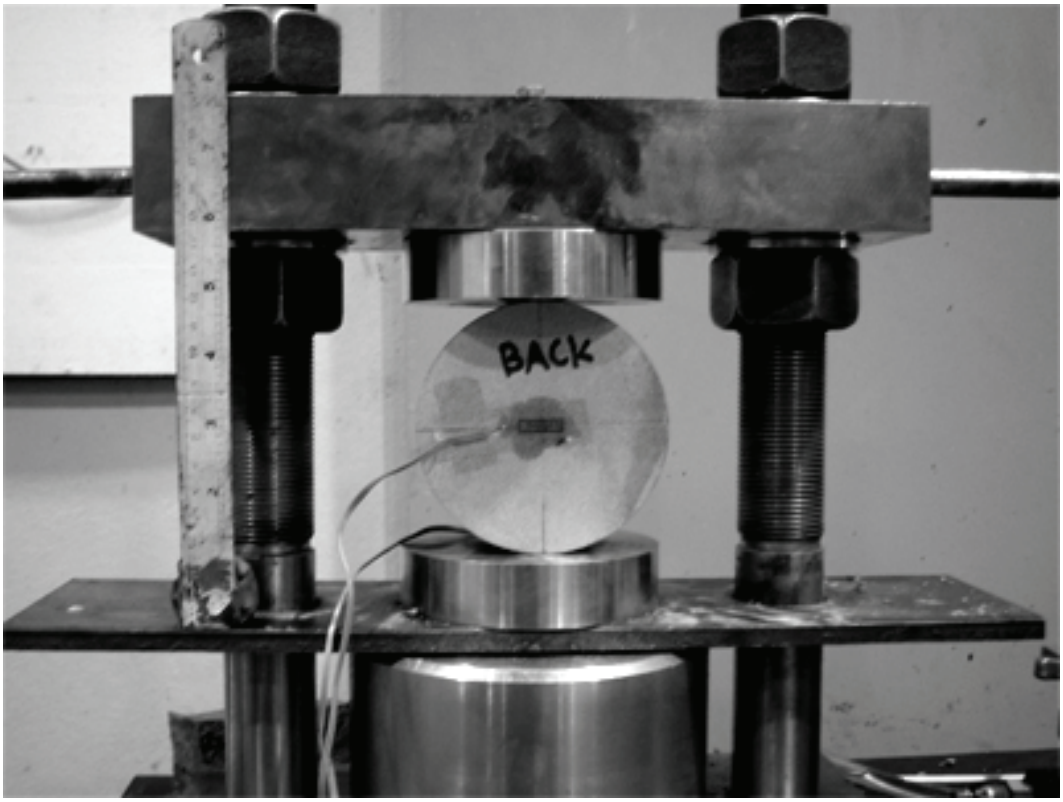

Figure 4.13 Brazilian test on 100 mm disk of sandstone during the strain measurements.

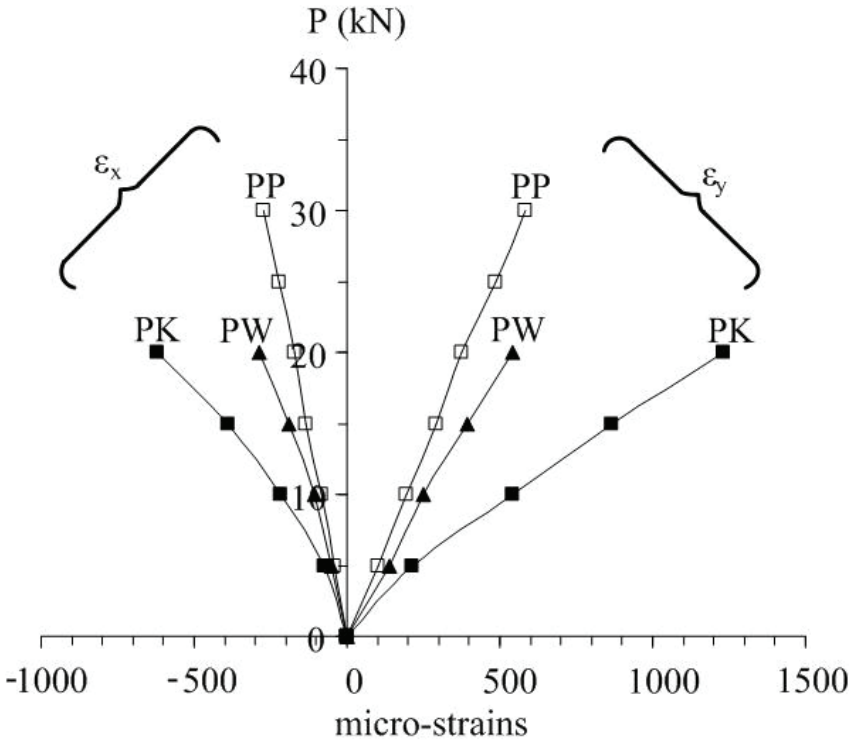

Figure 4.14 Strain measurement results from Brazilian testing on PP, PW and PK sandstones.

Table 4.1 Elastic properties in the direction normal and parallel to bedding planes.

	Rock Types	E_p (GPa)	E_n (GPa)	ν_p	ν_n
Uniaxial Compression Test	PW	10.3	N/A	N/A	N/A
	PP	11.1	N/A	N/A	N/A
	PK	10.1	N/A	N/A	N/A
Polyaxial Compression Test (Walsri et al, 2009)	PW	10.0	8.6	0.38	0.28
	PP	11.1	10.3	0.36	0.33
	PK	8.7	6.4	0.25	0.19
Brazilian Tension Test	PW	9.2	N/A	0.21	N/A
	PP	11.2	N/A	0.19	N/A
	PK	5.9	N/A	0.11	N/A

CHAPTER V

STRENGTH CRITERIA

5.1 Introduction

This chapter describes the strength analysis and criteria under tension. The results are compared with Coulomb and modified Wiebols and Cook failure criteria. They are selected because the Coulomb criterion has been widely used in actual field applications while the modified Wiebols and Cook criterion has been claimed by many researchers to be one of the best representations of rock strengths under confinement.

5.2 Analysis

The Coulomb and modified Wiebols and Cook failure criteria are used to describe the rock strengths when the minimum principal stress is in tension. First the results of the Brazilian tests under axial compression are calculated in terms of $J_2^{1/2}$ as a function of J_1. The induced horizontal tensile stress (σ_x) always represents the minimum principal stress (σ_3) in this test. Under low axial stress, the vertical compressive stress (σ_y) at the crack initiation point represents the maximum principal stress (σ_1), and the axial stress represents the intermediate principal stress (σ_2). When the axial stress is increased beyond a certain magnitude, σ_z becomes σ_1, and σ_y becomes σ_2.

5.3 Coulomb Criteria Prediction

The second order stress invariant ($J_2^{1/2}$) and the first order stress invariant or the mean stress (J_1) are calculated from the test results by the following relations (Jaeger & Cook, 1979):

$$J_2^{1/2} = \sqrt{(1/6)\{(\sigma_1 - \sigma_2)^2 + (\sigma_1 - \sigma_3)^2 + (\sigma_2 - \sigma_3)^2\}} \tag{5.1}$$

$$J_1 = (\sigma_1 + \sigma_2 + \sigma_3)/3 \tag{5.2}$$

The Coulomb criterion in from of J_2 and J_1 can be expressed as:

$$J_2^{1/2} = \frac{2}{\sqrt{3}}\left[J_1 \sin\varphi + S_0 \cos\varphi\right] \tag{5.3}$$

where φ is friction angle, S_o is cohesion, J_1 is mean stress and $J_2^{1/2}$ is the second order of stress invariant.

From the test results the stress invariant $J_2^{1/2}$ as a function of mean stress J_1 is compared with the predictions by the Coulomb criterion in (Figures 5.1 through 5.3) for PP, PW and PK sandstones. Since the Coulomb criterion ignores σ_2 at failure, the predicted $J_2^{1/2}$ is independent of J_1 for each σ_3. The predicted $J_2^{1/2}$ decreases with σ_3 when the applied axial stress (σ_z) represents σ_1, and increases with σ_3 when the induced vertical stress (σ_y) represents σ_1. These stress variations conform well to the actual test results. The Coulomb criterion over-estimates the actual strengths for all levels of σ_3. On average the discrepancies are about 15-20%.

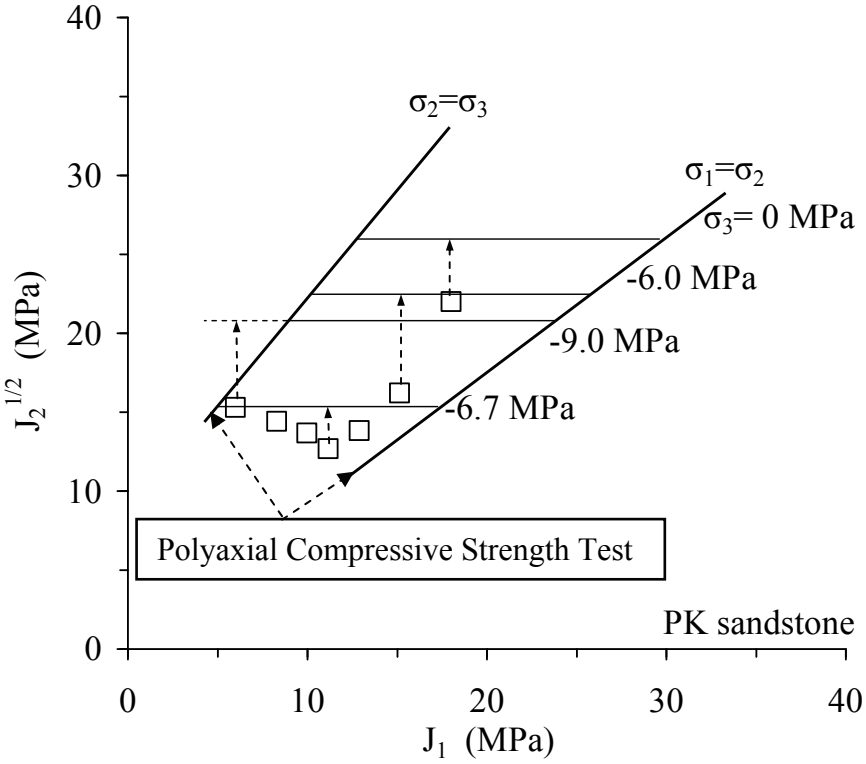

Figure 5.1 $J_2^{1/2}$ as a function of J_1 for Brazilian testing PK sandstones compared with the Coulomb criterion predictions.

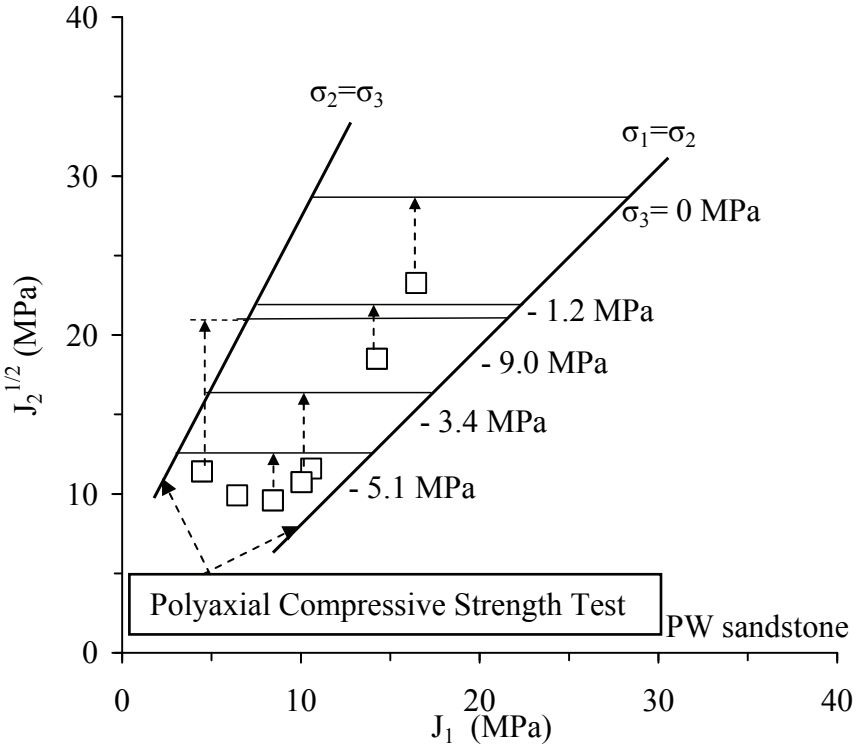

Figure 5.2 $J_2^{1/2}$ as a function of J_1 for Brazilian testing on PW sandstones compared with the Coulomb criterion predictions.

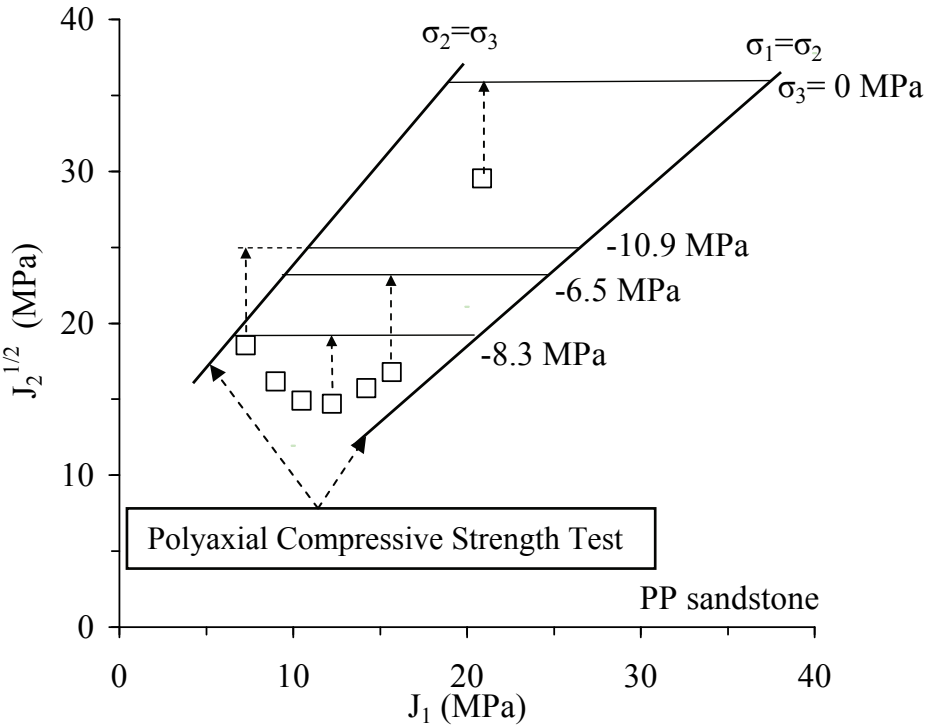

Figure 5.3 $J_2^{1/2}$ as a function of J_1 for Brazilian testing on PP sandstones compared with the Coulomb criterion predictions.

5.4 Modified Wiebols and Cook criteria prediction

The modified Wiebols and Cook criterion given by Colmenares & Zoback (2002) defines $J_2^{1/2}$ at failure in terms of J_1 as:

$$J_2^{1/2} = A + BJ_1 + CJ_1^2 \tag{5.4}$$

The constants A, B and C depend on rock materials and the minimum principal stresses (σ_3). They can be determined under the conditions where $\sigma_2 = \sigma_3$, as follows (Colmenares & Zoback, 2002):

$$C = \frac{\sqrt{27}}{2C_1 + (q-1)\sigma_3 - C_0} \times \left(\frac{C_1 + (q-1)\sigma_3 - C_0}{2C_1 + (2q+1)\sigma_3 - C_0} - \frac{q-1}{q+2} \right) \tag{5.5}$$

where: $C_1 = (1 + 0.6\mu_i)C_0$

C_0 = uniaxial compressive strength of the rock.

$\mu_i = \tan\phi$

$q = \{(\mu_i^2 + 1)^{1/2} + \mu_i\}^2 = \tan^2(\pi/4 + \phi/2)$

$$B = \frac{\sqrt{3}(q-1)}{q+2} - \frac{C}{3}(2C_0 + (q+2)\sigma_3 \tag{5.6}$$

$$A = \frac{C_0}{\sqrt{3}} - \frac{C_0}{3}B - \frac{C_0^2}{9}C \tag{5.7}$$

The comparison between the measured strengths with the predictions by the modified Wiebols and Cook criterion for the three sandstones (Figures 5.4 through

5.6). The criterion is not sensitive to the observed variations of the rock strengths in the $J_2^{1/2}$ - J_1 diagram. The predicted $J_2^{1/2}$ curves continue to decrease as the minimum stress decreases. This does not strictly reflect the actual observations where $J_2^{1/2}$ increases after the induced vertical stress becomes the maximum principal stress. It appears that the modified Wiebols and Cook criterion can not describe the rock strengths when the minimum principal stress is in tension.

5.5 Discussions of the test results

The Coulomb criterion performs better when the minimum principal stress is in tension. It can describe the decrease and increase of $J_2^{1/2}$ at failure due to the variation of the minimum principal tensile stresses with the discrepancy of about 15-20%. It is clear that the modified Wiebols and Cook criterion can not be correlated with the rock strengths when the minimum principal stress is in tension**.**

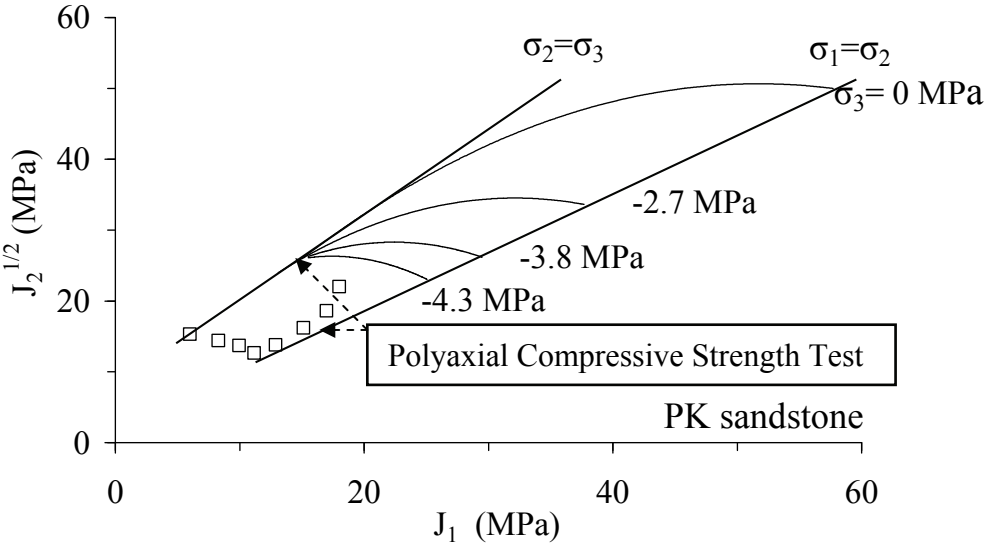

Figure 5.4 $J_2^{1/2}$ as a function of J_1 for Brazilian testing on PK sandstones compared with the modified Wiebols and Cook criterion.

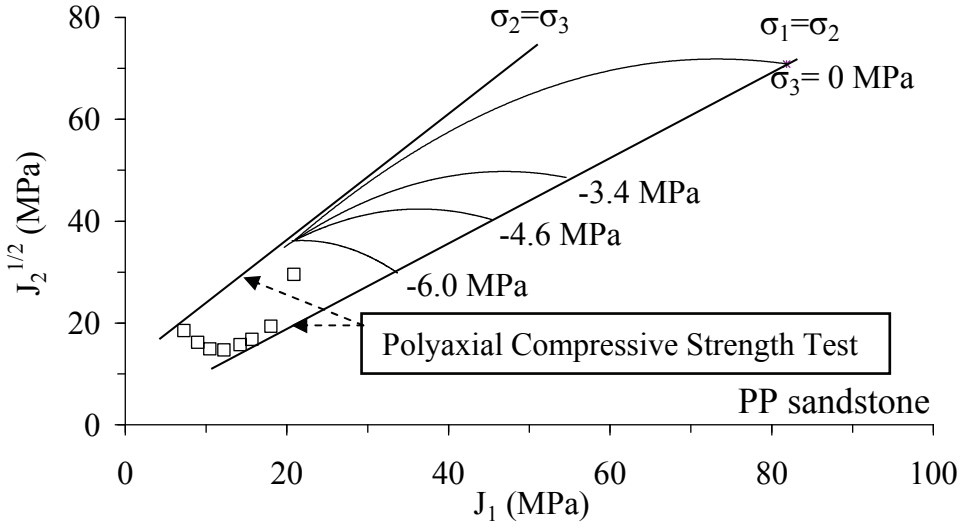

Figure 5.5 $J_2^{1/2}$ as a function of J_1 for Brazilian testing on PP sandstones compared with the modified Wiebols and Cook criterion.

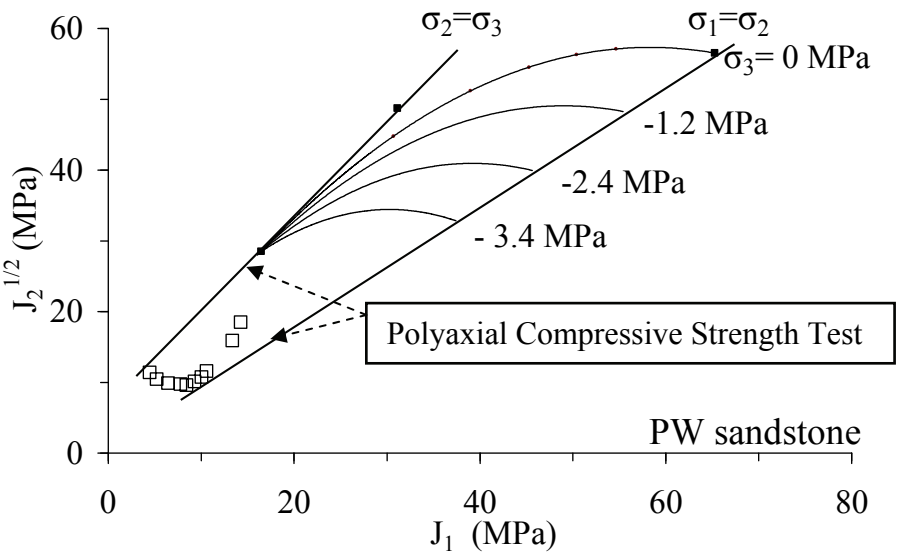

Figure 5.6 $J_2^{½}$ as a function of J_1 for Brazilian testing on PW sandstones compared with the modified Wiebols and Cook criterion.

CHAPTER VI

DISCUSSIONS, CONCLUSIONS, AND RECOMMENDATIONS FOR FUTURE STUDIES

6.1 Discussions and Conclusions

The results from Brazilian tension test under axial confinement can be postulated that the axial stress may cause tensile strains in the directions of σ_1 and σ_3. Due to the effect of the Poisson's ratio, σ_2 can produce tensile strains in the directions normal to its axis (or on the plane parallel to σ_1 and σ_3). These tensile strains increase from the minimum on the mid-section plane to the maximum on the specimen surfaces where the rock can freely dilate. These tensile strains cause splitting tensile fractures of the rock specimen. This is supported by the results of the Brazilian testing under axial compression. The applied σ_z produces a tensile strains adding to the line load-induced tensile stress at the specimen center. As a result a smaller magnitude of the line load is required to split the Brazilian specimen when it is under an axial compression. Based on this mechanism alone the higher the σ_2 that is applied, the lower σ_1 or $J_2^{1/2}$ is required to fail the specimen. Since the induced tensile strains by σ_2 in the polyaxial specimen is not uniformly distributed on the σ_1 - σ_3 plane, quantitative determination of the effect of σ_2 under this mechanism is not easy. The elastic properties under tension may differ from those in compression. The calculation is also complicated by the same mechanism induced by σ_1 and σ_3.

When σ_2 approaches σ_1 (i.e. high σ_2:σ_3 ratio or low σ_1:σ_2 ratio) the tensile strain induced by σ_2 becomes more pronounced and overcomes the strengthening rate. Under this condition, σ_1 at failure decreases with increasing σ_2, and the rock is failed by splitting tensile fractures. The proposed mechanisms can explain why at a given σ_3, σ_1 at failure initially increases with σ_2 when σ_2 is low. This phenomenon is particularly obvious when σ_3 is very low. It is recommended that rock deformation properties be incorporated into a failure criterion to fully describe the rock tensile strengths under confinements. Deserving special attention is the derivation of a strain energy-based criterion which can take both the principal stresses and principal strains (or elastic properties) at failure into consideration.

From the test results the stress invariant $J_2^{1/2}$ as a function of mean stress J_1 is compared with the predictions by the Coulomb and modified Wiebols and Cook criterion. The Coulomb criterion performs better when the minimum principal stress is in tension. It can describe the decrease and increase of $J_2^{1/2}$ at failure due to the variation of the minimum principal tensile stresses with the discrepancy of about 15-20%. It is clear that the modified Wiebols and Cook criterion can not be correlated with the rock strengths when the minimum principal stress is in tension.

The findings from this research have improved our understanding of the rock tensile strength under a more complex stress state than those usually obtained from the conventional (e.g. direct tension test, beam bending test, and Brazilian tension test). It is clear that the intermediate principal stress even in compression can significant reduce the rock tensile strength. Recognition of this effect is of particular important for the stability analysis of roof beam of underground openings and tunnels. Application of the rock tensile strength, determined from the conventional Brazilian

tension test method, to the actual condition may result in a non-conservative analysis. The effect of the intermediate principal stress, normally parallel to the tunnel or opening axis, shall be taken into consideration.

6.2 Recommendations for future studies

The uncertainties and adequacies of the research investigation and results discussed above lead to the recommendations for further studies, as follows.

A more testing is required to assess the effect of the intermediate principal stress. Studying of size effect and a variety of rocks with a broad range of strengths and elasticity should be tested. This is to confirm the reliability of the Coulomb criterion under the condition where one or two of the principal stress is in tension. The effects of pore pressure on the rock tensile strengths and elasticity is also desirable. Result from a variety of test configurations, for example four-point beam and ring tension tests with axial compression shall be compared and analyzed under multi-axial strength criterion.

REFERENCES

ASTM D3967-95a. Standard Test Methods Splitting Tensile Strength of Intact Rock Core Specimens. **Annual Book of ASTM Standards** Vol. 04.08. Philadelphia: American Society for Testing and Materials.

Amadei, B., Rogers, J. D. and Goodman, R. E. (1983). Elastic constants and tensile strength of the anisotropic rocks. **Proceedings of the Fifth Congress of International Society of Rock Mechanics**, Melbourne. Rotterdam: Balkema. pp 189–196.

Brown, E.T. (1981). Rock Characterization testing and Monitoring : ISRM Suggested Methods. New York: **International Society for Rock Mechanics**, Pergamon Press.

Cai, M. (2007). Influence of intermediate principal stress on rock fracturing and strength near excavation boundaries – Insight from numerical modeling, **International Journal of Rock Mechanics & Mining**. Vol. 45 : 269-772.

Chen, C.S., Pan, E. and Amadei, B. (1998). Determination of deformability and tensile strength of anisotropic rock using Brazilian tests. **International Journal of Rock Mechanics & Mining**. Vol. 35(1) : 43-61.

Claesson, J. and Bohloli, B. (2002). Brazilian test: stress field and tensile strength of anisotropic rocks using an analytical solution. **International Journal of Rock Mechanics & Mining Sciences**. Vol. 39 : 991-1004.

Colmenares, L. B., and Zoback, M. D. (2002). A statistical evaluation of intact rock failure criteria constrained by polyaxial test data for five different rocks. **International Journal of Rock Mechanics & Mining Sciences 39.** USA, pp. 695-729.

Diederichs, M.S., and Kaiser P.K. (1999). Tensile strength and abutment relaxation as failure control mechanisms in underground excavations. **International Journal of Rock Mechanics & Mining**. Vol. 36 : 69-96.

Fuenkajorn, K. and Daemen, J. J. K. (1986). **Experimental Assessment of Borehole Wall Drilling Damage in Basalt Rock**. U.S. Nuclear Regulatory Commission. pp 58-77.

Haimson, B. (2006). True Triaxial Stresses and the Brittle Fracture of Rock. **Pure and Applied Geophysics.** Vol. 163 : 1101–1113.

Hondros, G. (1959). The evaluation of Poisson's ratio and the modulus of materials of low tensile resistance by the Brazilian (indirect tensile) tests with particular reference to concrete. **Australian Journal of Applied Sciences.** Vol. 10 : 243-268.

Jaeger, J. C. and Cook, N. W. (1979). **Fundamentals of Rock Mechanic**. London: Chapman and Hall. pp 169-173.

Jianhong, Y., Wu, F.Q., and Sun, J.Z. (2008). Estimation of the tensile elastic modulus using Brazilian disc by applying diametrically opposed concentrated loads. **International Journal of Rock Mechanics & Mining**. Vol. 46(3) : 568-576.

Lanaro, F., Sato, T., and Stephansson, O. (2009). Microcrack modelling of Brazilian tensile tests with the boundary element method. **International Journal of Rock Mechanics & Mining**. Vol. 46 : 450-461.

Liao, J. J., Yang, M. T. and Hsieh, H. Y. (1997). Direct tensile behavior of a transversely isotropic rock, **International Journal of Rock Mechanics & Mining Sciences**. Vol. 34(5) : 831-849.

Ohokal, M., Funatol, A. and Takahashi, Y. (1997). Tensile test using hollow cylindrical specimen **International Journal of Rock Mechanics & Mining Sciences**. Vol. 34(3-4) : 1997 ISSN 0148-9062.

Singh, B., Goel, R. K., Mehrotra, V. K., Garg, S. K. and Allu, M. R. (1998). Effect of Intermediate Principal Stress on Strength of Anisotropic Rock Mass, **Tunnelling and Underground Space Technology**. Vol. 13(1) : 71-79.

Tepnarong, P. (2001). Theoretical and Experimental Studies to Determine Compressive and Tensile Strength of Rock, Using Modified Point Load Testing. **M.S. Thesis**, Suranaree University of Technology, Thailand.

Tien, Y.M., Kuo, M.C., and Juang, C.H. (2006). An experimental investigation of the failure mechanism of simulated transversely isotropic rocks. **International Journal of Rock Mechanics & Mining**. Vol. 43 : 1163-1181.

Wang, Q.Z., Jia, X.M, Kou, S.Q., Zhang, Z.X., and Lindqvist, P.A. (2003). The flattened Brazilian disc specimen used for testing elastic modulus, tensile strength and fracture toughness of brittle rocks: analytical and numerical results. **International Journal of Rock Mechanics & Mining**. Vol. 41 : 245-253.

Wang, Q.Z., Li, W., and Xie, H.P. (2009). Dynamic split tensile test of Flattened Brazilian Disc of rock with SHPB setup. **Mechanics of Materials**. Vol. 41 : 252–260.

Walsri, C., Poonprakon, P., Thosuwan, R., and Fuenkajorn, K. (2009). Compressive and tensile strengths of sandstones under true triaxial stresses. **Proceedings of The second Thailand Symposium on Rock Mechanics**, Thailand, pp 199-218.

Wijk, G. (1978). Some new theoretical aspects of indirect measurements of tensile strength of rock. **International Journal of Rock Mechanics & Mining Sciences**. Abstr. 15: 149-160.

APPENDIX A

LIST OF PUBLICATIONS

Rock Mechanics, Fuenkajorn & Phien-wej (eds) © 2009. ISBN 978 974 533 624 7

Compressive and tensile strengths of sandstones under true triaxial stresses

C. Walsri, P. Poonprakon, R. Thosuwan & K. Fuenkajorn
Geomechanics Research Unit, Suranaree University of Technology, Thailand

Keywords: True triaxial, polyaxial, intermediate principal stress, sandstone, anisotropic

ABSTRACT: A polyaxial load frame has been developed to determine the compressive and tensile strengths of three types of sandstone under true triaxial stresses. Results from the polyaxial compression tests on rectangular specimens of sandstones suggest that the rocks are transversely isotropic. The measured elastic modulus in the direction parallel to the bedding planes is slightly greater than that normal to the bedding. Poisson's ratio on the plane normal to the bedding planes is lower than those on the parallel ones. Under the same σ_3, σ_1 at failure increases with σ_2. Results from the Brazilian tension tests under axial compression reveal the effects of the intermediate principal stress on the rock tensile strength. The Coulomb and modified Wiebols and Cook failure criteria derived from the characterization test results predict the sandstone strengths in term of $J_2^{1/2}$ as a function of J_1 under true triaxial stresses. The modified Wiebols and Cook criterion describes the failure stresses better than does the Coulomb criterion when all principal stresses are in compressions. When the minimum principal stresses are in tension, the Coulomb criterion over-estimate the second order of the stress invariant at failure by about 20% while the modified Wiebols and Cook criterion fails to describe the rock tensile strengths.

1 INTRODUCTION

The effects of confining pressures at great depths on the mechanical properties of rocks are commonly simulated in a laboratory by performing triaxial compression testing of cylindrical rock core specimens. A significant limitation of these conventional methods is that the intermediate and minimum principal stresses are equal during the test while the actual in-situ rock is normally subjected to an anisotropic stress state where the maximum, intermediate and minimum principal stresses are different ($\sigma_1 \neq \sigma_2 \neq \sigma_3$). It has been commonly found that compressive strengths obtained from conventional triaxial testing can not represent the actual in-situ strength where the rock is subjected to an anisotropic stress state (Yang et al., 2007; Haimson, 2006; Tiwari & Rao, 2004, 2006; Haimson & Chang, 1999). A variety of devices have been developed for rock testing under true triaxial stresses. Some recent ones include those proposed by Reddy et al. (1992), Smart (1995), Wawersik et al. (1997), Haimson & Chang (2000), and Alexeev et al. (2004). These devices are mostly designed for testing rock specimens under compression.

From the experimental results on brittle rocks obtained by the researchers above (e.g., Colmenares & Zoback, 2002; Haimson, 2006) it can be generally concluded that in a σ_1 - σ_2 diagram, for a given σ_3, σ_1 at failure initially increases with σ_2 to a certain magnitude, and then it gradually decreases as σ_2 increases. The effect of σ_2 is more pronounced under higher σ_3. Cai (2008) offers an explanation of how the intermediate principal stress affects the rock strength based on the results from numerical simulations on fracture initiation and propagation. He states that the intermediate principal stress confines the rock in such a way that fractures can only be initiated and propagated in the direction parallel to σ_1 and σ_2. The effect of σ_2 is related to the stress-induced anisotropic properties and behavior of the rock and to the end effect at the interface between the rock surface and loading platen in the direction of σ_2 application. The effect should be smaller in homogeneous and fine-grained rocks than in coarse-grained rocks where pre-existing micro-cracks are not uniformly distributed.

Several failure criteria have been developed to describe the rock strength under true triaxial stress states. Comprehensive reviews of these criteria have been given recently by Colmenares & Zoback (2002), Al-Ajmi & Zimmerman (2005), Haimson (2006), Benz & Schwab (2008), Cai (2008), Haimson & Hudson (2008) and You (2008). Among several other criteria, the Mogi and modified Wiebols and Cook criteria are perhaps the most widely used to describe the rock compressive strengths under true triaxial stresses. These strength criteria however have rarely been verified when one or two of the principal stresses are in tension. Obtaining rock strengths under an anisotropic stress state is not only difficult but expensive. A special loading device (e.g., polyaxial loading machine or true triaxial load cell) is required. As a result test data under true triaxial stress conditions have been relatively limited. Most researchers above have used the same sets of test data (some obtained over a decade ago) to compare with their new numerical simulations, field observations (notably on breakout of deep boreholes) or to verify their new strength criteria and concepts. Due to the cost and equipment availability for obtaining true triaxial strengths, in common engineering practices application of a failure criterion that can incorporate the three-dimensional stresses has been very rare.

This research involves the development of a simple and low-cost polyaxial load frame to test rock specimens under true triaxial stress states. The frame performance is assessed by conducting polyaxial compression tests and Brazilian tension tests under axial compression to study the deformation and failure characteristics of sandstone specimens. The Coulomb and modified Wiebols and Cook failure criteria derived from the results of conventional tests are used to describe the compressive and tensile strengths of the rocks under true triaxial stress states.

2 ROCK SAMPLES

The tested sandstones are from three sources: Phu Phan, Phra Wihan and Phu Kradung formations (hereafter designated as PP, PW and PK sandstones). These fine-grained quartz sandstones are selected primarily because of their highly uniform texture, density and strength. Their average grain size is 0.1-1.0 mm. They are commonly found in the north and northeast of Thailand. Their mechanical properties and responses play a significant role in the stability of tunnels, slope embankments and dam foundations in the region. For the polyaxial compression testing rectangular block specimens are cut and ground to have a nominal dimension of 5×5×10 cm. The perpendicularity and parallelism of the specimens follow the ASTM (D 4543) specifications. The longest axis is parallel to the bedding planes and to the direction of the major principal stress. Though having different shape the

Rock Mechanics, Fuenkajorn & Phien-wej (eds) © 2009. ISBN 978 974 533 624 7

specimens used here have volume and length-to-diameter ratio comparable to those used in the conventional uniaxial and triaxial compression test methods. The Brazilian tension test uses disk specimens with a nominal diameter of 50 mm with a thickness-to-diameter ratio of 0.5 to comply with ASTM D 3967-95. The core axis is normal to the bedding planes. All specimens are oven-dried before testing.

3 POLYAXIAL LOAD FRAME

The development of the polyaxial load frame is based on three key design requirements: (1) capable of maintaining constant lateral stresses (σ_2 and σ_3) during the test, (2) capable of testing specimen with volume equal to or larger than those used in the conventional triaxial testing, and (3) allowing monitoring of specimen deformation along the principal axes. Figure 1 shows the polyaxial load frame developed in this research. To meet the load requirement above, two pairs of cantilever beams are used to apply the lateral stresses in mutually perpendicular directions to the rock specimen. The outer end of each opposite beam is pulled down by dead weight placed in the middle of a steel bar linking the two opposite beams underneath (Figure 2). The inner end is hinged by a pin mounted on vertical bars on each side of the frame. During testing all beams are arranged perfectly horizontally, and hence a lateral compressive load results on the specimen placed at the center of the frame. Due to the different distances from the pin to the outer weighting point and from the pin to the inner loading point, a load magnification of 17 to 1 is obtained from load calibration with an electronic load cell. This loading ratio is also used to determine the lateral deformation of the specimen by monitoring the vertical movement of the two steel bars below. The maximum lateral load is designed for 100 kN. The axial load is applied by a 1000-kN hydraulic load cell. The load frame can accommodate specimen sizes from 2.5×2.5×2.5 cm to 10×10×20 cm. The different specimen sizes and shapes can be tested by adjusting the distances between the opposite loading platens. Note that virtually all true triaxial and polyaxial cells previously developed elsewhere can test rock samples with the maximum size not larger than 5×5×10 cm.

4 POLYAXIAL COMPRESSION TESTS

The polyaxial compression tests are performed to determine the compressive strengths and deformations of the PK, PP and PW sandstones under true triaxial stresses. The intermediate (σ_2) and minimum (σ_3) principal stresses are maintained constant while σ_1 is increased until failure. Here the constant σ_2 is varied from 0 to 17 MPa, and σ_3 from 0 to 6 MPa. Neoprene sheets are used to minimize the friction at all interfaces between the loading platen and the rock surface. Figure 3 shows the applied principal stress directions with respect to the bedding planes for all specimens. The measured sample deformations are used to determine the strains along the principal axes during loading. The failure stresses are recorded and mode of failure examined.

4.1 Test Results

Figure 4 plots the stress-strain curves from the start of loading to failure for some sandstone specimens. The elastic modulus and Poisson's ratio are calculated for the directions normal and parallel to the bedding planes. Under the stress orientation used here where σ_1 and σ_2 are parallel to the bedding planes, the three-dimensional principal stress-strain relations given by Jaeger & Cook (1979) can be simplified to obtain a set of governing equations for a transversely isotropic material as:

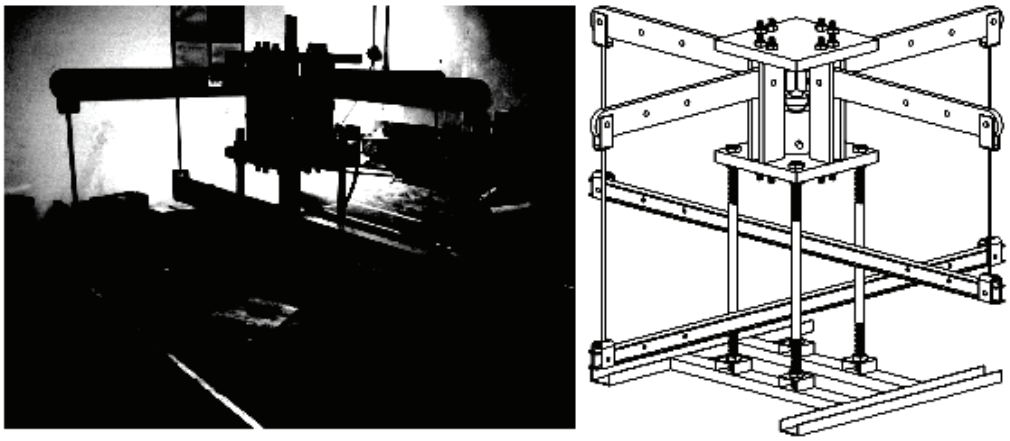

Figure 1. Polyaxial load frame developed for compressive and tensile strength testing under true triaxial stress.

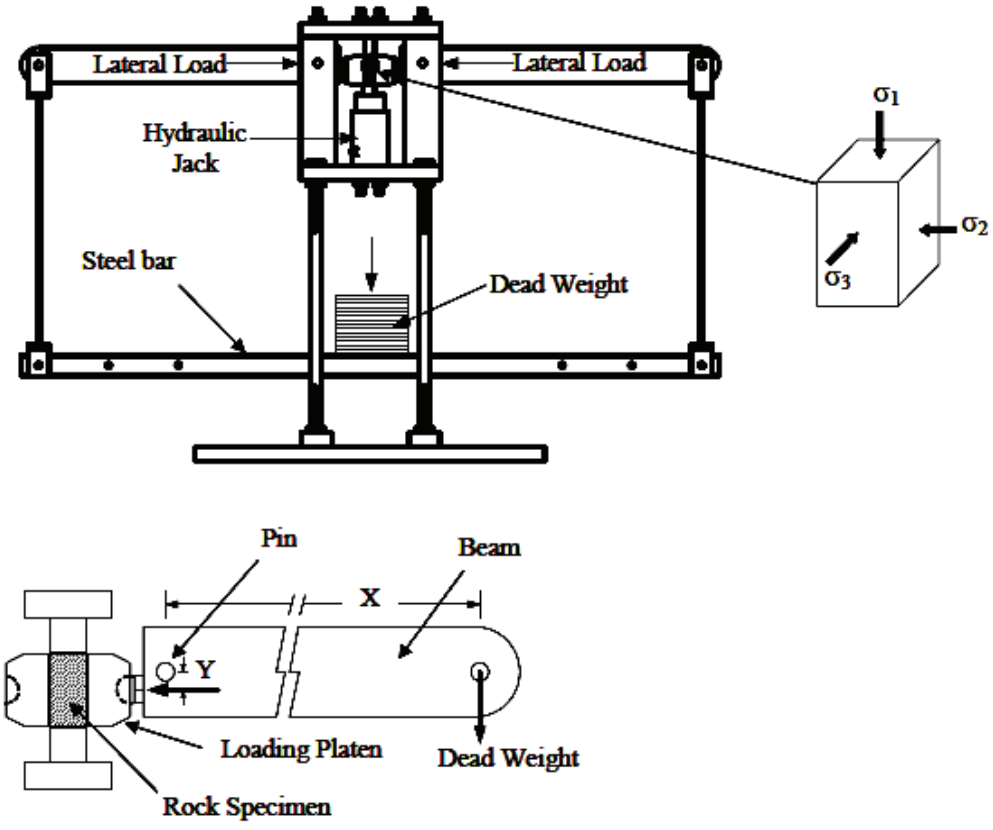

Figure 2. Cantilever beam weighed at outer end applies lateral stress to the rock specimen.

Rock Mechanics, Fuenkajorn & Phien-wej (eds) © 2009. ISBN 978 974 533 624 7

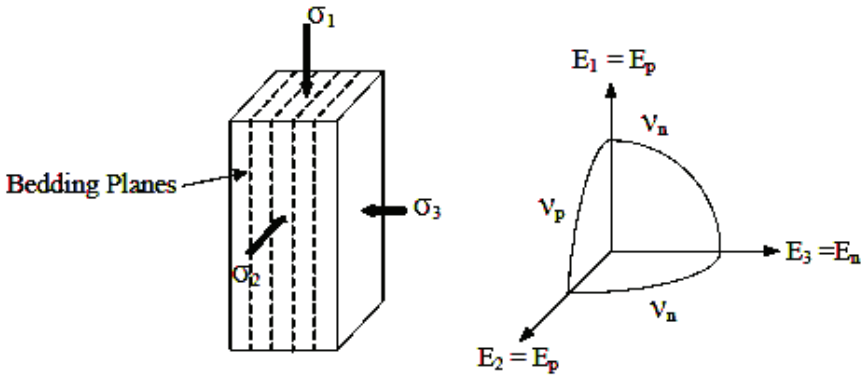

Figure 3. Directions of loading with respect to the bedding planes (left). Elastic parameters for transversely isotropic conditions (right).

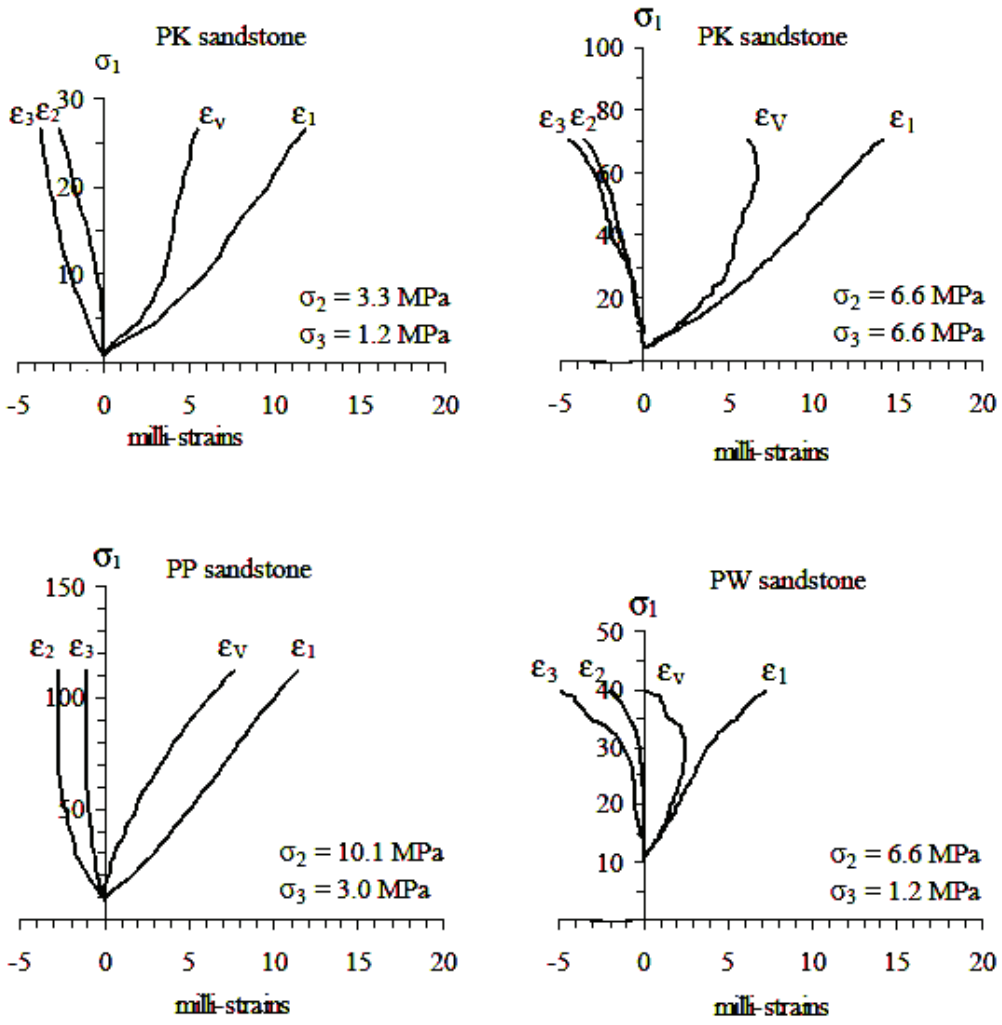

Figure 4. Examples of stress-strain curves of the three sandstones under polyaxial loading.

$$\varepsilon_1 = \frac{\sigma_1}{E_p} - \frac{\sigma_2 \nu_p}{E_p} - \frac{\sigma_3 \nu_n}{E_n} \quad (1)$$

$$\varepsilon_2 = -\frac{\sigma_1 \nu_p}{E_p} + \frac{\sigma_2}{E_p} - \frac{\sigma_3 \nu_n}{E_n} \quad (2)$$

$$\varepsilon_3 = -\frac{\sigma_1 \nu_n}{E_p} - \frac{\sigma_2 \nu_n}{E_p} + \frac{\sigma_3}{E_n} \quad (3)$$

where: σ_1, σ_2 and σ_3 are principal stresses, ε_1, ε_2 and ε_3 are principal strains, E_n and E_p are elastic moduli normal and parallel to the bedding planes, and ν_n and ν_p are Poisson's ratio's on the planes normal and parallel to the bedding.

The calculations of the Poisson's ratios and tangent elastic moduli are made at 50% of the maximum principal stress. The PW and PP sandstones exhibit a small transversely isotropic behavior. The elastic modulus in the direction normal to the bedding planes is slightly lower than that parallel to the bedding planes. The Poisson's ratio on the plane parallel to the beds is less than that across the beds. Table 1 summarizes the elastic parameters with respect to the bedding plane orientation.

Figure 5 plots σ_1 at failure as a function of σ_2 tested under various σ_3's for the PW and PP sandstones. The results show the effects of the intermediate principal stress, σ_2, on the maximum stresses at failure by the failure envelopes being offset from the condition where $\sigma_2 = \sigma_3$. For all minimum principal stress levels, σ_1 at failure increases with σ_2. The effect of σ_2 tends to be more pronounced under a greater σ_3. These observations agree with those obtained elsewhere (e.g. Haimson & Chang, 2000; Colmenares & Zoback, 2002; Haimson, 2006). Post-failure observations suggest that compressive shear failures are predominant in the specimens tested under low σ_2 while splitting tensile fractures parallel to σ_1 and σ_2 directions dominate under higher σ_2 (Figure 6). The observed splitting tensile fractures under relatively high σ_2 suggest that the fracture initiation has no influence from the friction at the loading interface in the σ_2 direction. As a result the increase of σ_1 with σ_2 should not be due to the interface friction. This does not agree with a conclusion drawn by Cai (2008) that friction at the interface in the σ_2 direction contributes to the increase of σ_1 at failure. Under the conditions when $\sigma_2 = \sigma_3$, the magnitudes of σ_1 at failure agree well with the triaxial compressive strength test results obtained by Kenkhunthod and Fuenkajorn (2009).

4.2 Strength Criteria

The Coulomb and modified Wiebols and Cook failure criteria are used to describe the polyaxial strengths of the PW and PP sandstones. They are selected because the Coulomb criterion has been widely used in actual field applications while the modified Wiebols and Cook criterion has been claimed by many researchers to be one of the best representations of rock strengths under polyaxial compression. To represent the rock strengths under true triaxial stresses the second order stress invariant ($J_2^{1/2}$) and the first order stress invariant or the mean stress (J_1) are calculated from the test results by the following relations (Jaeger & Cook, 1979):

$$J_2^{1/2} = \sqrt{(1/6)\{(\sigma_1 - \sigma_2)^2 + (\sigma_1 - \sigma_3)^2 + (\sigma_2 - \sigma_3)^2\}} \quad (4)$$

Rock Mechanics, Fuenkajorn & Phien-wej (eds) © 2009. ISBN 978 974 533 624 7

Table 1. Elastic properties in the direction normal and parallel to bedding planes.

	Rock Types	E_p (GPa)	E_n (GPa)	ν_p	ν_n
Polyaxial Compression Test	PW	10.0	8.6	0.38	0.28
	PP	11.1	10.3	0.36	0.33
Brazilian Tension Test	PW	9.2	N/A	0.21	N/A
	PP	14.8	N/A	0.19	N/A
	PK	5.9	N/A	0.11	N/A

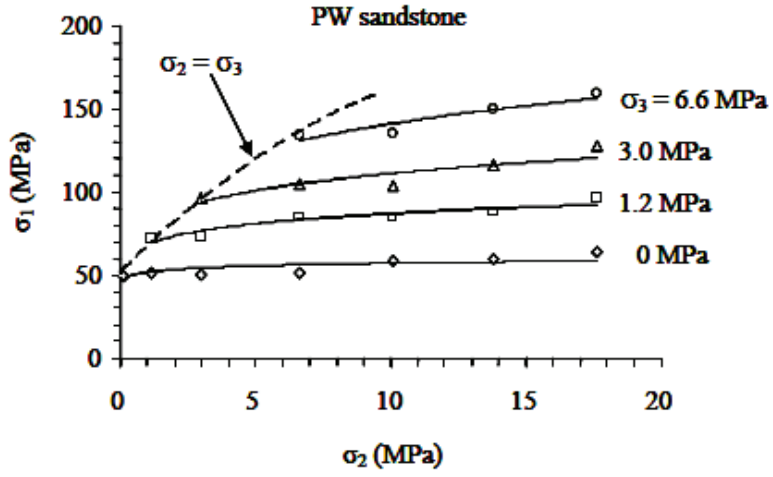

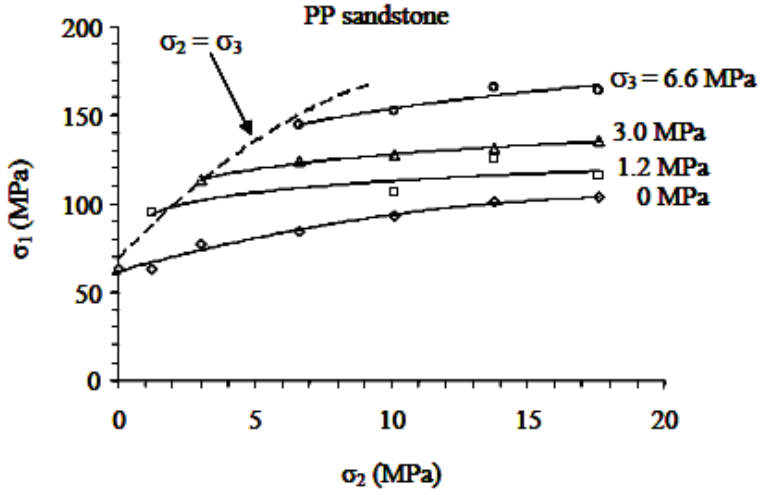

Figure 5. Maximum principal stress (σ_1) at failure as a function of σ_2 for various σ_3 values.

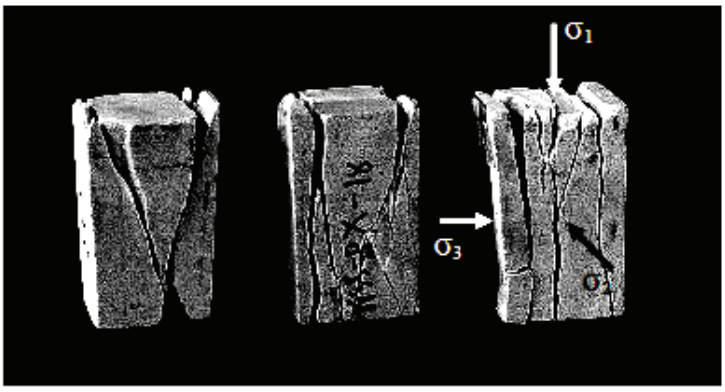

Figure 6. Post-tested specimens of PW sandstone. Left: $\sigma_1 = 51$, $\sigma_2 = 1.2$, $\sigma_3 = 0$ MPa. Middle: $\sigma_1 = 50$, $\sigma_2 = 3.0$, $\sigma_3 = 0$ MPa. Right: $\sigma_1 = 58.8$, $\sigma_2 = 10.0$, $\sigma_3 = 0$ MPa.

$$J_1 = (\sigma_1 + \sigma_2 + \sigma_3)/3 \tag{5}$$

Here the Coulomb criterion is derived from the uniaxial and triaxial compressive strengths of the rocks where σ_2 and σ_3 are equal. Figures 7 and 8 compare the polyaxial test results with those predicted by the Coulomb criterion for PW and PP sandstones. The predictions are made for σ_3 = 0, 1.2, 3.0 and 6.6 MPa (as used in the tests) and under stress conditions from $\sigma_2 = \sigma_3$ to $\sigma_1 = \sigma_2$. In the $J_2^{1/2}$ - J_1 diagram, $J_2^{1/2}$ increases with σ_3 but it is independent of J_1 because the Coulomb criterion ignores σ_2 in the strength calculation. Under a low σ_2 and σ_3 the Coulomb prediction tends to agree with the test results obtained from the PW sandstone. Except for this case, no correlation between the Coulomb predictions and the polyaxial strengths can be found. The inadequacy of the predictability of Coulomb criterion under polyaxial stress states obtained here agrees with a conclusion drawn by Colmenares & Zoback (2002).

The modified Wiebols and Cook criterion given by Colmenares & Zoback (2002) defines $J_2^{1/2}$ at failure in terms of J_1 as:

$$J_2^{1/2} = A + BJ_1 + CJ_1^2 \tag{6}$$

The constants A, B and C depend on rock materials and the minimum principal stresses (σ_3). They can be determined under the conditions where $\sigma_2 = \sigma_3$, as follows (Colmenares & Zoback, 2002):

$$C = \frac{\sqrt{27}}{2C_1 + (q-1)\sigma_3 - C_0} \times \left(\frac{C_1 + (q-1)\sigma_3 - C_0}{2C_1 + (2q+1)\sigma_3 - C_0} - \frac{q-1}{q+2} \right) \tag{7}$$

where: $C_1 = (1 + 0.6\mu_i)C_0$ (8)

C_0 = uniaxial compressive strength of the rock.

$\mu_i = \tan\phi$ (9)

$q = \{(\mu_i^2 + 1)^{1/2} + \mu_i\}^2 = \tan^2(\pi/4 + \phi/2)$ (10)

$$B = \frac{\sqrt{3}(q-1)}{q+2} - \frac{C}{3}(2C_0 + (q+2)\sigma_3 \tag{11}$$

Rock Mechanics, Fuenkajorn & Phien-wej (eds) © 2009. ISBN 978 974 533 624 7

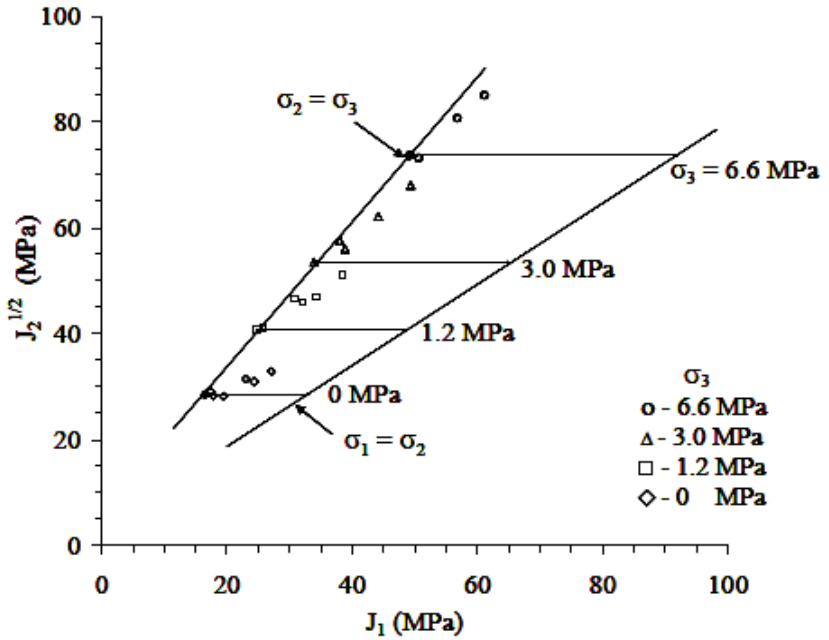

Figure 7. $J_2^{1/2}$ as a function of J_1 from testing PW sandstone compared with the Coulomb criterion predictions (lines).

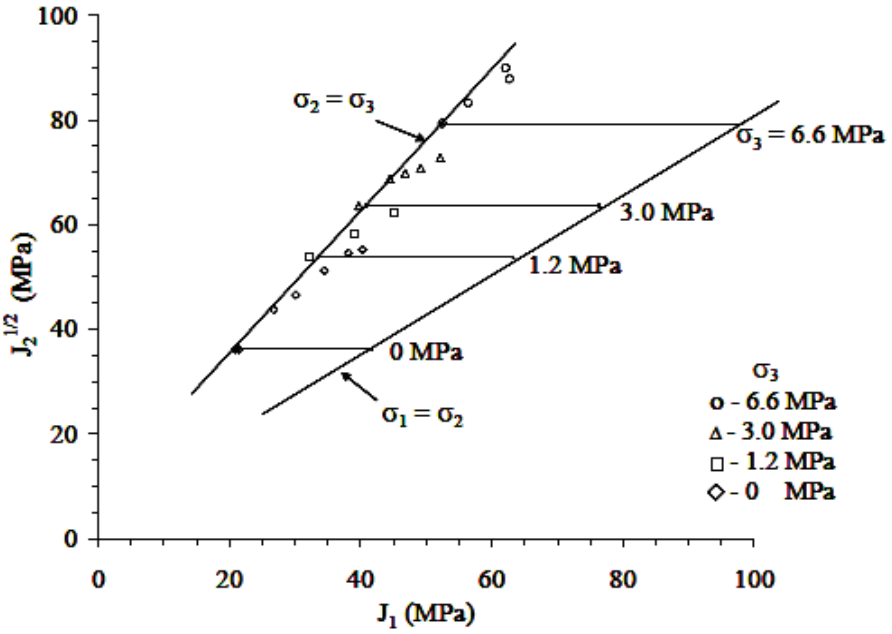

Figure 8. $J_2^{1/2}$ as a function of J_1 from testing PP sandstone compared with the Coulomb criterion predictions (lines).

$$A = \frac{C_0}{\sqrt{3}} - \frac{C_0}{3}B - \frac{C_0^2}{9}C \qquad (12)$$

The numerical values for A, B and C for PW and PP sandstones are given in Table 2 for each σ_3 tested here. Substituting these constants into equation (6), the upper and lower limits of $J_2^{1/2}$ for each rock type can be defined under conditions of $\sigma_2 = \sigma_3$ and $\sigma_1 = \sigma_2$. The predictions are made for σ_3 = 0, 1.2, 3.0 and 6.6 MPa. Figures 9 and 10 compare the test results with those predicted by the modified Wiebols and Cook criterion. The predictions tend to be higher than the sandstone strengths under low σ_3. Under a higher σ_3 the criterion well represents the polyaxial strengths of the rocks. This conforms to the results obtained by Colmenares & Zoback (2002) that predictive capability of the modified Wiebols and Cook criterion improves as the minimum principal stress increases.

5 BRAZILIAN TENSION TESTS UNDER AXIAL COMPRESSION

The Brazilian tension tests with axial compression have been performed on PP, PW and PK sandstone disks to determine the effects of the intermediate principal stress on the rock tensile strength. The polyaxial load frame is used to apply a constant axial stress on the disk specimen while the diametral line load is increased until failure (Figure 11). The constant axial stress is varied from zero (Brazilian test) to as high as the rock compressive strength. Neoprene sheets are used to minimize the friction between the rock surface and loading platen in the axial direction.

5.1 Brazilian Tension Test Results

Figure 12 plots the line load at failure (P_f) as a function of the axial stress (σ_z) for the three sandstones. The failure load linearly decreases with increasing axial stress. At $P_f = 0$ the axial stress becomes the uniaxial compressive strength of the rock. The tensile stresses (σ_x) and compressive stresses (σ_y) induced at the crack initiation point in the middle of the specimen also decrease with increasing axial stress (Figure 13). These stresses are calculated from the solutions given by Jaeger & Cook (1979). The test results reveal a linear transition from the Brazilian tensile strength to the uniaxial compressive strength, which can be best demonstrated by using Mohr's circles, as shown in Figure 14.

Post-failure observations show that under low σ_z a single splitting extension crack along the loading diameter is normally induced in the disk specimen. Multiple extension cracks are developed as σ_z increase. When σ_z reaches the uniaxial compressive strength of the rocks, the specimens fail without applying the diametral line load. At this point the specimens are crushed, resulting in multiple shear fractures and extension cracks (Figure 15). It is postulated that the axial stress produces tensile strains perpendicular to its direction due to the effect of the Poisson's ratio. At the crack initiation point this tensile strain is combined with

Table 2. Parameters A, B and C for PW and PP sandstones.

Rock types	PW Sandstone				PP Sandstone			
σ_3 (MPa)	0	1.2	3.0	6.6	0	1.2	3.0	6.6
A (MPa)	1.37	0.54	-0.41	-1.7	1.97	1.16	0.17	-1.2
B	1.92	1.94	1.96	1.99	1.91	1.92	1.94	1.96
C (MPa^{-1})	-0.016	-0.014	-0.012	-0.009	-0.013	-0.013	-0.01	-0.008

Rock Mechanics, Fuenkajorn & Phien-wej (eds) © 2009. ISBN 978 974 533 624 7

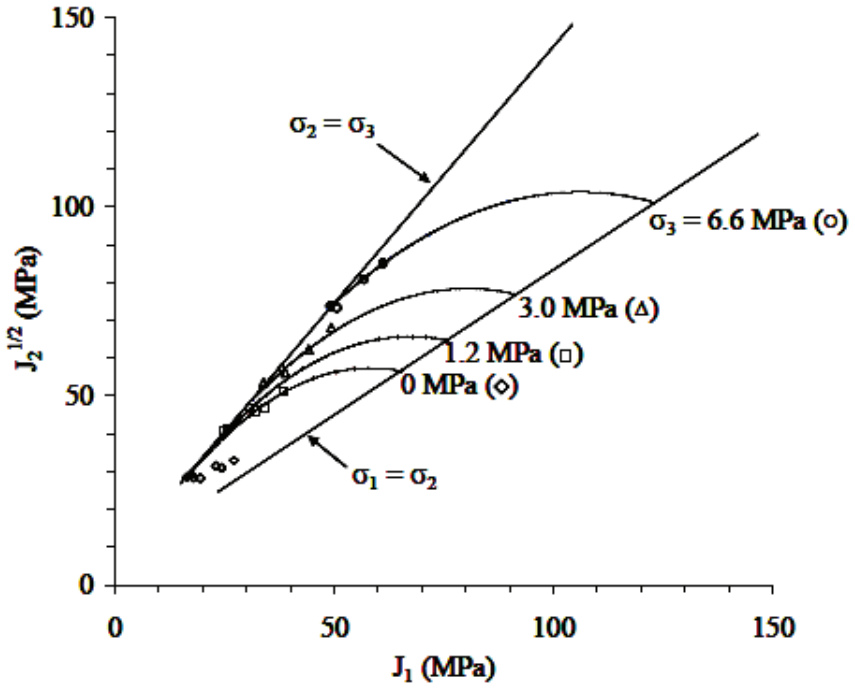

Figure 9. $J_2^{1/2}$ as a function of J_1 from testing PW sandstone compared with the modified Wiebols and Cook criterion predictions (lines).

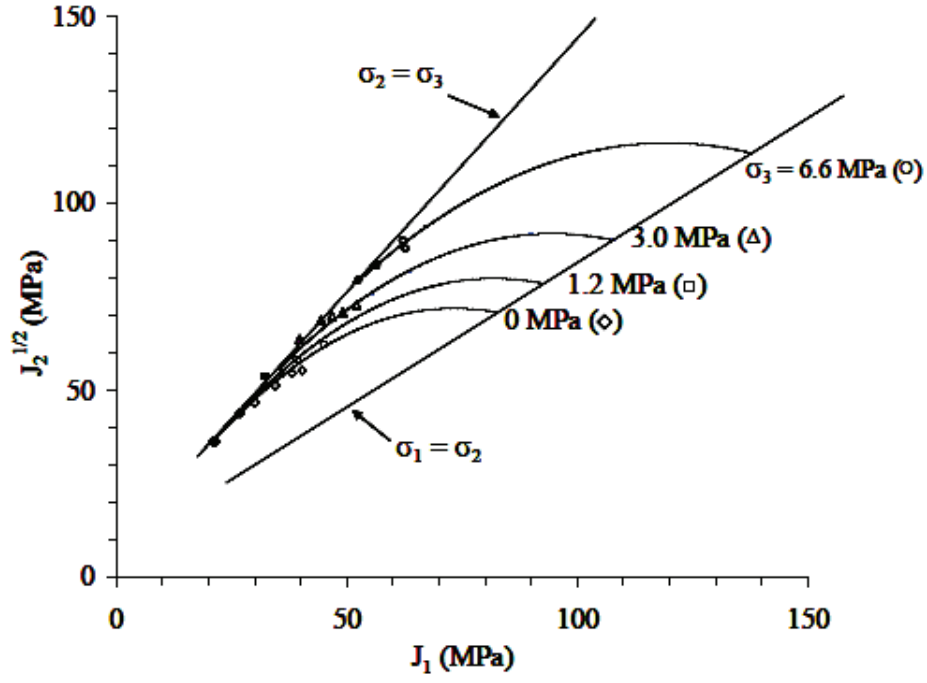

Figure 10. $J_2^{1/2}$ as a function of J_1 from testing PP sandstone compared with the modified Wiebols and Cook criterion predictions (lines).

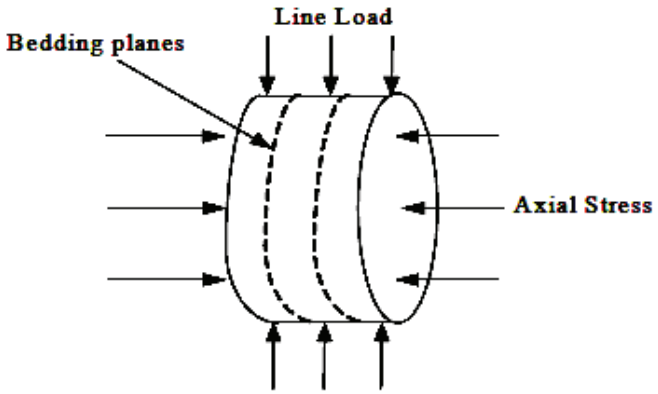

Figure 11. Brazilian tension test specimen under axial compression.

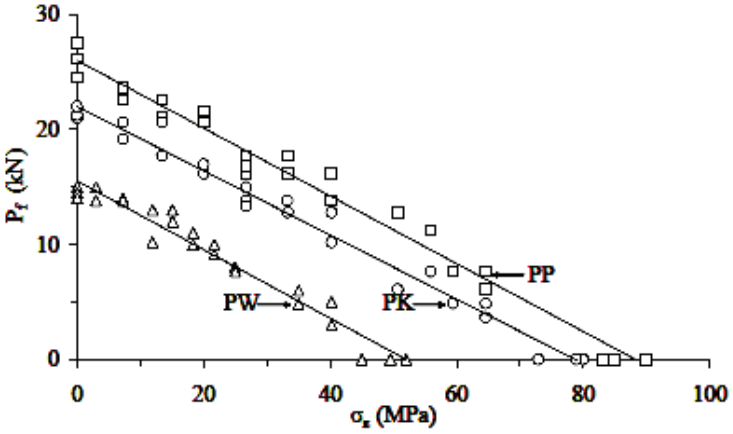

Figure 12. Line load at failure (P_f) as a function of applied axial stress (σ_z).

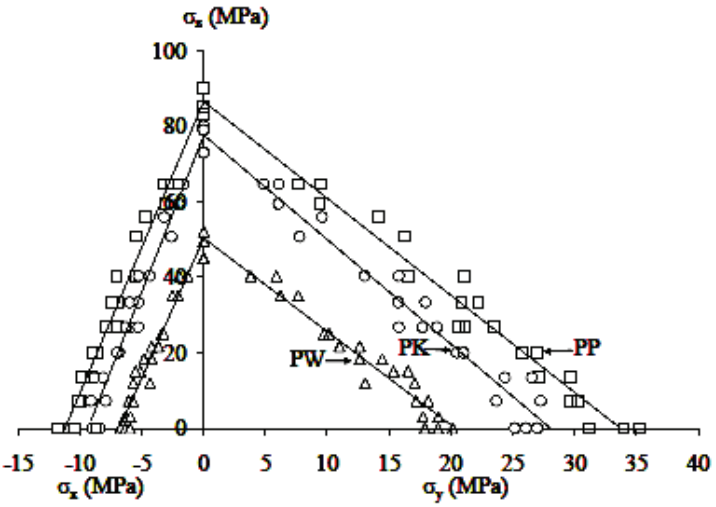

Figure 13. Induced compressive (σ_y) and tensile stresses (σ_x) at failure as a function of applied σ_z.

Rock Mechanics, Fuenkajorn & Phien-wej (eds) © 2009. ISBN 978 974 533 624 7

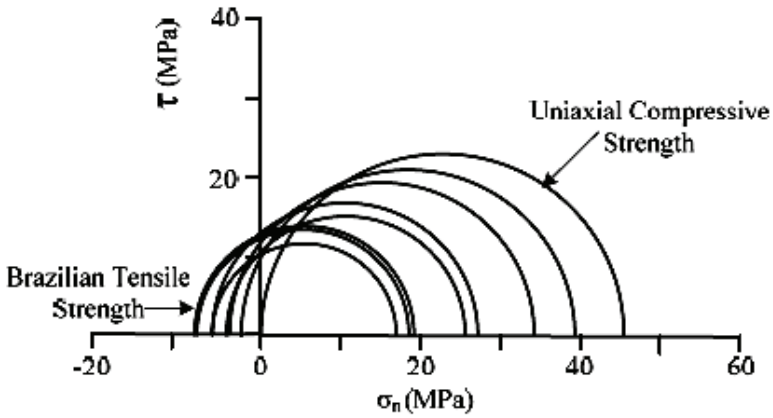

Figure 14. Mohr's circles from testing of PW sandstone showing transition from Brazilian tensile strength to uniaxial compressive strength.

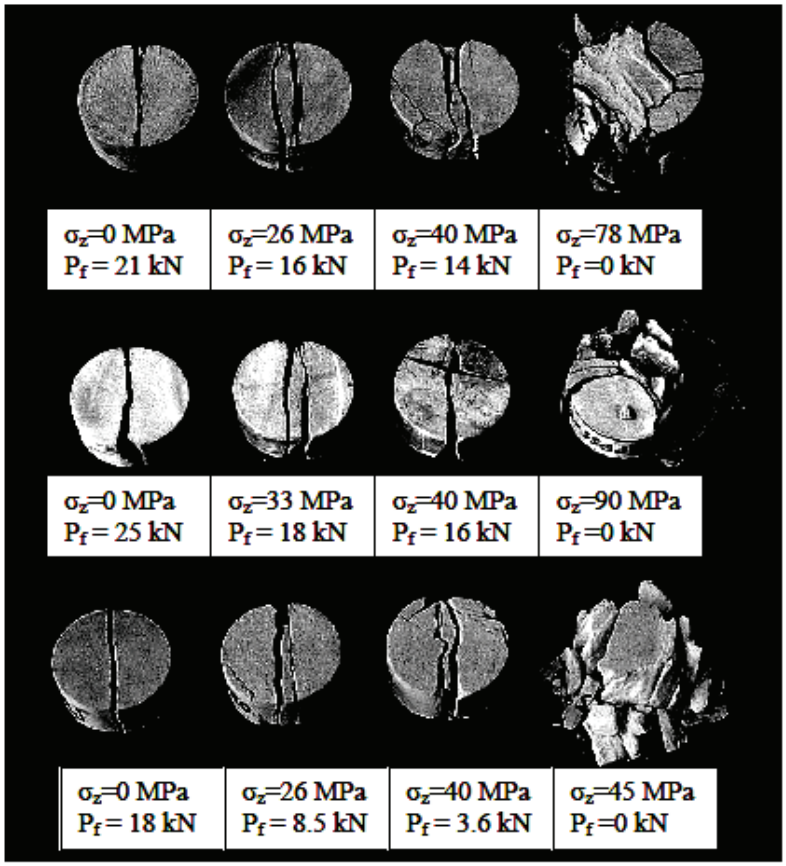

Figure 15. Some post- test specimens of PK sandstone (top), PP sandstone (middle) and PW sandstone (bottom).

the horizontal tensile stress that is induced by the line load. The line load at failure therefore decreases with increasing σ_z. Calculation of the σ_z-induced tensile strain for the entire specimen is however not that simple because the rock is under both tension and compression and the elastic properties under tension and compression may be different (Jaeger & Cook, 1979; Chen et al., 1998). More discussion on this issue is given in the next section.

Under no axial stress the elastic modulus and Poisson's ratio of the sandstones are measured by installing strain gages at the center of the sandstone specimen. The gages measure the vertical compressive strain, ε_y, (along the loading diameter) and horizontal tensile strain, ε_x, induced during line loading. Three samples have been tested for each rock type. Figure 16 plots the measured strains as a function of the applied load, P. The elastic modulus and Poisson's ratio can be calculated using the following equations (Hondros, 1959):

$$\nu = -\frac{3\varepsilon_x + \varepsilon_y}{3\varepsilon_y + \varepsilon_x} \tag{13}$$

$$E = \frac{2P(1-\nu)^2}{\pi Dt(\varepsilon_x + \nu\varepsilon_y)} \tag{14}$$

These equations assume that the rock is linearly elastic and isotropic and that the elastic modulus in tension is equal to that in compression. The E and ν above are compared with those obtained from the polyaxial compression testing in Table 1. Since all Brazilian disks are prepared to have bedding planes normal to the disk axis, only elastic modulus and Poisson's ratio parallel to the bedding can be measured. The discrepancy of the elastic parameters obtained from the two test types may be because the rock elastic modulus under tension is lower than that under compression and there is intrinsic variability among the tested specimens.

5.2 Strength Criteria under Tension

The Coulomb and modified Wiebols and Cook failure criteria are used to describe the rock strengths when the minimum principal stress is in tension. First the results of the Brazilian tests under axial compression are calculated in terms of $J_2^{1/2}$ as a function of J_1. The induced horizontal tensile stress (σ_x) always represents the minimum principal stress (σ_3) in this test. Under low axial stress, the vertical compressive stress (σ_y) at the crack initiation point represents the maximum principal stress (σ_1), and the axial stress represents the intermediate principal stress (σ_2). When the axial stress is increased beyond a certain magnitude, σ_z becomes σ_1, and σ_y becomes σ_2.

From the test results the stress invariant $J_2^{1/2}$ as a function of mean stress J_1 is compared with the predictions by the Coulomb criterion in Figure 17 for PP, PW and PK sandstones. Since the Coulomb criterion ignores σ_2 at failure, the predicted $J_2^{1/2}$ is independent of J_1 for each σ_3. The predicted $J_2^{1/2}$ decreases with σ_3 when the applied axial stress (σ_z) represents σ_1, and increases with σ_3 when the induced vertical stress (σ_y) represents σ_1. These stress variations conform well to the actual test results. The Coulomb criterion over-estimates the actual strengths for all levels of σ_3. On average the discrepancies are about 15-20%.

Rock Mechanics, Fuenkajorn & Phien-wej (eds) © 2009. ISBN 978 974 533 624 7

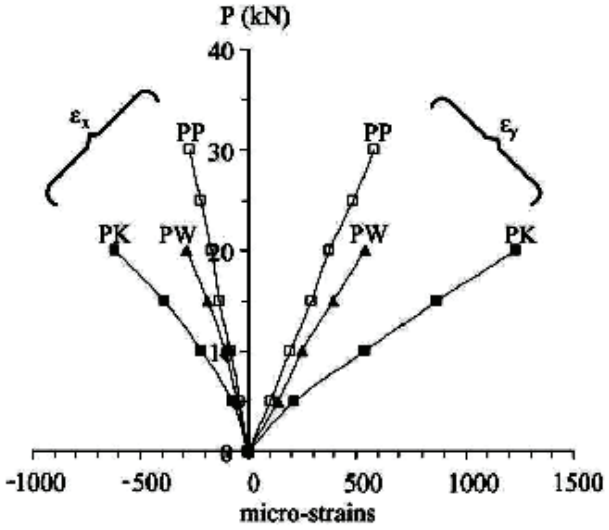

Figure 16. Strain measurements from Brazilian testing on PP, PW and PK sandstones.

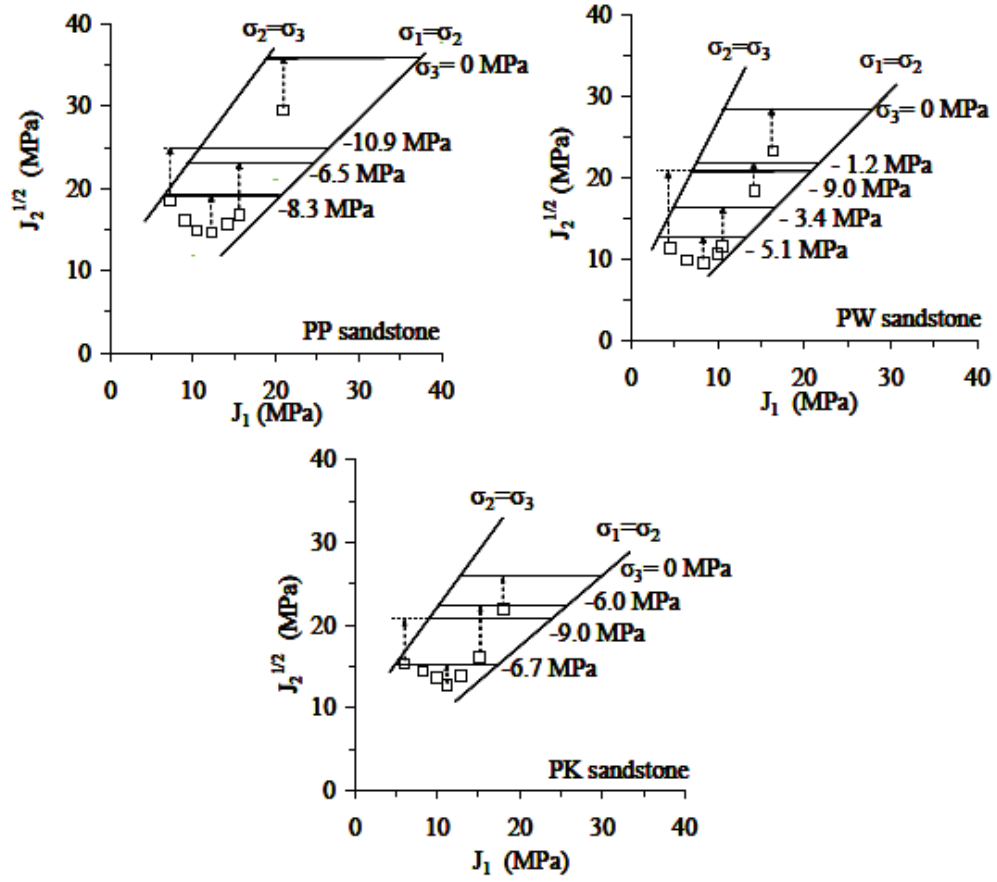

Figure 17. $J_2^{1/2}$ as a function of J_1 for Brazilian testing on PP, PW and PK sandstones compared with the Coulomb criterion predictions.

Figure 18 compares the measured strengths with the predictions by the modified Wiebols and Cook criterion for the three sandstones. The criterion is not sensitive to the observed variations of the rock strengths in the $J_2^{1/2}$ - J_1 diagram. The predicted $J_2^{1/2}$ curves continue to decrease as the minimum stress decreases. This does not strictly reflect the actual observations where $J_2^{1/2}$ increases after the induced vertical stress becomes the maximum principal stress. It appears that the modified Wiebols and Cook criterion can not describe the rock strengths when the minimum principal stress is in tension.

7 DISSCUSSIONS AND CONCLUSIONS

The invented polyaxial load frame performs well for the assessment of the effects of σ_2 on the compressive and tensile strengths of the sandstones. Measuring the specimen deformations by monitoring the movement of the cantilever beams is sufficiently accurate and sensitive to detect the transversely isotropic behavior of the PW and PP sandstones. An advantage of the polyaxial frame is that it can test rock specimens with a wider range of sizes and shapes as compared to most true triaxial cells previously developed. Such flexibility allows us to perform a variety of test configurations, for example polyaxial creep testing, four-point beam bending tests with lateral confinement, Brazilian and ring tension tests with axial compression, and borehole stability testing under biaxial and polyaxial stresses.

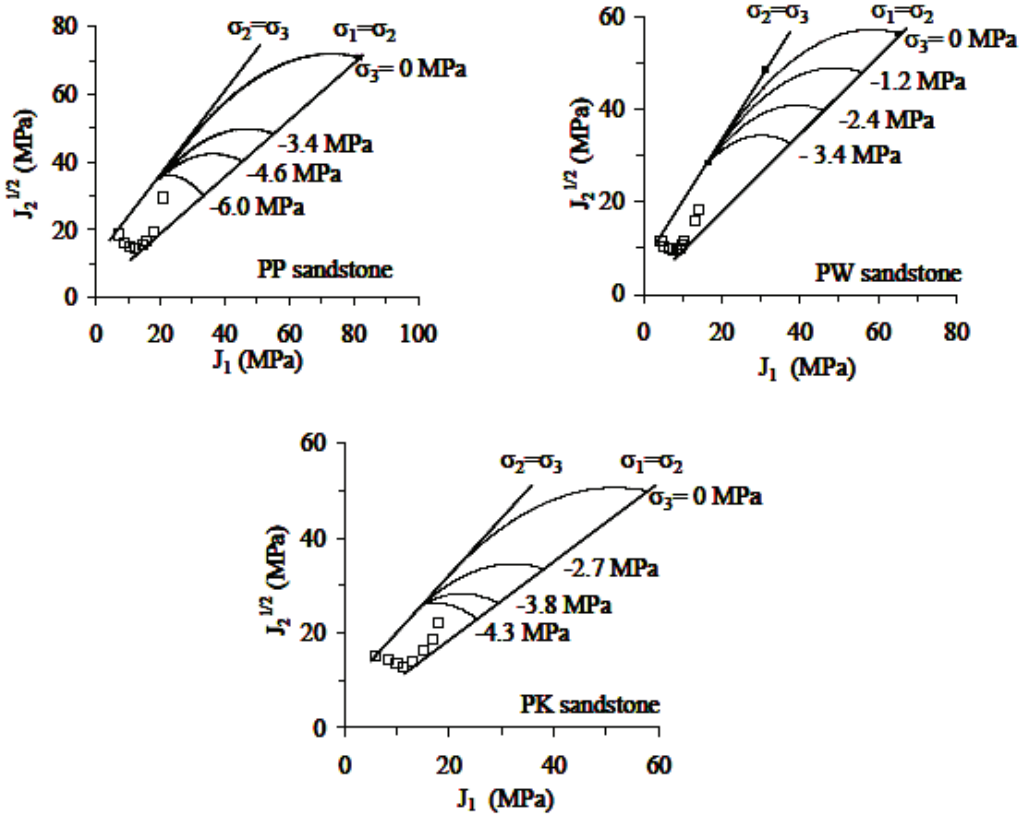

Figure 18. $J_2^{1/2}$ as a function of J_1 for Brazilian testing on PP, PW and PK sandstones compared with the modified Wiebols and Cook criterion.

Rock Mechanics, Fuenkajorn & Phien-wej (eds) © 2009. ISBN 978 974 533 624 7

Neoprene sheets used here can effectively reduce the friction between the rock surface and loading platen, as evidenced by the fact that σ_1 at failure measured under $\sigma_2 = \sigma_3$ for these sandstones is comparable to the corresponding triaxial compressive strengths of the rocks obtained by the conventional method (Kenkhunthod & Fuenkajorn, 2009). It can be concluded that the interface friction did not contribute to the increase of σ_1 at failure under true triaxial testing as suggested by Cai (2008).

Under true triaxial compressive stresses the modified Wiebols and Cook criterion can predict the compressive strengths of the tested sandstones reasonably well. Due to the effect of σ_2 the Coulomb criterion can not represent the rock strengths under true triaxial compressions, particularly under high σ_2 to σ_3 ratios. The Coulomb criterion however performs better when the minimum principal stress is in tension. It can describe the decrease and increase of $J_2^{1/2}$ at failure due to the variation of the minimum principal tensile stresses with the discrepancy of about 15-20%. It is clear that the modified Wiebols and Cook criterion can not be correlated with the rock strengths when the minimum principal stress is in tension

It is postulated that the effects of the intermediate principal stress are caused by two mechanisms working simultaneously but having opposite effects on the rock polyaxial strengths; (1) mechanism that strengthens the rock matrix in the direction normal to σ_1 - σ_3 plane, and (2) mechanism that induces tensile strains in the directions of σ_1 and σ_3.

The intermediate principal stress can strengthen the rock matrix on the plane normal to its direction, and hence a higher differential stress is required to induce failure. This is simply the same effect obtained when applying a confining pressure to a cylindrical specimen in the conventional triaxial compression testing. Considering this effect alone, the higher the magnitude of σ_2 applied, the higher σ_1 (or $J_2^{1/2}$) is required to fail the specimen. Nevertheless it is believed that the relationship between σ_2 magnitudes and the degrees of strengthening can be non-linear, particularly under high σ_2. Such relation depends on rock types and their texture (e.g., distribution of grain sizes, pore spaces, fissures and micro-cracks, and types of rock-forming minerals).

At the same time due to effect of the Poisson's ratio σ_2 can produce tensile strains in the directions normal to its axis (or on the plane parallel to σ_1 and σ_3). These tensile strains increase from the minimum on the mid-section plane to the maximum on the specimen surfaces where the rock can freely dilate. These tensile strains cause splitting tensile fractures of the rock specimen. This is supported by the results of the Brazilian testing under axial compression. The applied σ_z produces a tensile strains adding to the line load-induced tensile stress at the specimen center. As a result a smaller magnitude of the line load is required to split the Brazilian specimen when it is under an axial compression. Based on this mechanism alone the higher the σ_2 that is applied, the lower σ_1 or $J_2^{1/2}$ is required to fail the specimen. Since the induced tensile strains by σ_2 in the polyaxial specimen is not uniformly distributed on the σ_1 - σ_3 plane, quantitative determination of the effect of σ_2 under this mechanism is not easy. The elastic properties under tension may differ from those in compression. The calculation is also complicated by the same mechanism induced by σ_1 and σ_3. Nevertheless it is suggested that the rock polyaxial strength is governed not only by the magnitudes of the three principal stresses, but also by its deformation properties.

The two mechanisms work simultaneously during polyaxial loading but with different degrees of influence depending on the magnitudes of the principal stresses at failure and of the rock elastic properties. When σ_2 is close to σ_3 (i.e. low σ_2:σ_3 ratio or high σ_1:σ_2 ratio) the

rock is strengthened by the increase of σ_2. Under this condition, the strengthening mechanism dominates, and σ_1 at failure increases with σ_2. Here the rock fails under compressive shear mode because the tensile strain induced by σ_2 is small. The rate of rock strengthening however decreases as σ_2 increases. When σ_2 approaches σ_1 (i.e. high σ_2:σ_3 ratio or low σ_1:σ_2 ratio) the tensile strain induced by σ_2 becomes more pronounced and overcomes the strengthening rate. Under this condition, σ_1 at failure decreases with increasing σ_2, and the rock is failed by splitting tensile fractures. The different modes of failure obtained under different stress conditions have been observed from the test results here. Between the two extreme conditions above the combined effects from the two mechanisms will determine the rock polyaxial strengths and its failure characteristics. For the polyaxial strength results obtained here and elsewhere (e.g. Colmenares & Zoback, 2002; Haimson, 2006; and You, 2008) the proposed mechanisms can explain why at a given σ_3, σ_1 at failure initially increases with σ_2 when σ_2 is low, and decreases with increasing σ_2 when σ_2 becomes larger. This phenomenon is particularly obvious when σ_3 is very low. It is recommended that rock deformation properties be incorporated into a failure criterion to fully describe the rock strengths under true triaxial stresses. Deserving special attention is the derivation of a strain energy-based criterion which can take both the principal stresses and principal strains (or elastic properties) at failure into consideration.

ACKNOWLEDGTMENT

This research is funded by Suranaree University of Technology. Permission to publish this paper is gratefully acknowledged.

REFERENCES

Al-Ajmi, A.M. & Zimmerman, R.W., 2005. Relation between the Mogi and the Coulomb failure criteria. *International Journal of Rock Mechanics & Mining Sciences*. 42:431-439.

Al-Ajmi, A.M. & Zimmerman, R.W., 2005. Relation between the Mogi and the Coulomb failure criteria. *International Journal of Rock Mechanics & Mining Sciences*. 42: 431-439.

Alexeev, A.D., Revva, V.N., Alyshev, N.A. & Zhitlyonok, D.M., 2004. True triaxial loading apparatus and its application to coal outburst prediction. *International Journal of Coal Geology*. 58: 245-250.

Alexeev, A.D., Revva, V.N., Alyshevb, N.A. & Zhitlyonok, D.M., 2004. True triaxial loading apparatus and its application to coal outburst prediction. *International Journal of Coal Geology*. 58: 245-250.

ASTM D3967-95. Standard Test Method for Splitting Tensile Strength of Intact Rock Core Specimens. *Annual Book of ASTM Standards*. 04.08. American Society for Testing and Materials: Philadelphia.

ASTM D3967-95. Standard Test Method for Splitting Tensile Strength of Intact Rock Core Specimens. *Annual Book of ASTM Standards*. 04.08. American Society for Testing and Materials, Philadelphia.

ASTM D4543-85. Standard Practice for Preparing Rock Core Specimens and Determining Dimensional and Shape Tolerances. *Annual Book of ASTM Standards*. 04.08. American Society for Testing and Materials: Philadelphia.

ASTM D4543-85. Standard Practice for Preparing Rock Core Specimens and Determining Dimensional and Shape Tolerances. *Annual Book of ASTM Standards*. 04.08. American Society for Testing and Materials, Philadelphia.

Benz, T. & Schwab, R., 2008. A quantitative comparison of six rock failure criteria. *International Journal of Rock Mechanics and Mining Sciences*. 45: 1176-1186.

Rock Mechanics, Fuenkajorn & Phien-wej (eds) © 2009. ISBN 978 974 533 624 7

Cai, M., 2007. Influence of intermediate principal stress on rock fracturing and strength near excavation boundaries—Insight from numerical modeling, *International Journal of Rock Mechanics & Mining Sciences*. 45:269-772.

Cai, M., 2008. Influence of intermediate principal stress on rock fracturing and strength near excavation boundaries—Insight from numerical modeling, *International Journal of Rock Mechanics & Mining Sciences*. 45: 763-772.

Chang, C. & Haimson, B., 2005. Non-dilatants deformation and failure mechanism in two Long Valley Caldera rocks under true triaxial compression. *International Journal of Rock Mechanics & Mining Sciences*. 42: 402-414.

Chang, C. & Haimson, B., 2005. Non-dilatants deformation and failure mechanism in two Long Valley Caldera rocks under true triaxial compression. *International Journal of Rock Mechanics & Mining Sciences*. 42: 402-414.

Chen, C. H., Pan, E. & Amadei B., 1998. Determination of the deformability and tensile strength of anisotropic rocks using Brazilian tests. *International Journal of Rock Mechanics & Mining Sciences*. 35: 43-61.

Chen, C. H., Pan, E. & Amadei B., 1998. Determination of the Deformability and Tensile Strength of Anisotropic Rocks Using Brazilian tests. *International Journal of Rock Mechanics & Mining Sciences*. 35: 43-61.

Claesson, J. & Bohloli, B., 2002. Brazilian test: stress field and tensile strength of anisotropic rocks using an analytical solution. *International Journal of Rock Mechanics & Mining Sciences*.

Colmenares, L.B. & Zoback, M.D., 2002. A statistical evaluation of intact rock failure criteria constrained by polyaxial test data for five different rocks. *International Journal of Rock Mechanics & Mining Sciences*. 39: 695-729.

Colmenares, L.B. & Zoback, M.D., 2002. A statistical evaluation of intact rock failure criteria constrained by polyaxial test data for five different rocks. *International Journal of Rock Mechanics & Mining Sciences*. 39: 695-729.

Haimson, B. & Chang, C., 1999. A new true triaxial cell for testing mechanical properties of rock, and its use to determine rock strength and deformability of Westerly granite. *International Journal of Rock Mechanics and Mining Sciences*. 37: 285-296.

Haimson, B. & Chang, C., 2000. A new true triaxial cell for testing mechanical properties of rock, and its use to determine rock strength and deformability of Westerly granite. *International Journal of Rock Mechanics and Mining Sciences*. 37: 285-296.

Haimson, B., 2006. True triaxial stresses and the brittle fracture of rock. *Pure and Applied Geophysics*. 163: 1101-1113.

Haimson, B., 2006. True Triaxial Stresses and the Brittle Fracture of Rock. *Pure and Applied Geophysics*. 163: 1101-1113.

Hondros, G., 1959. The evaluation of Poisson's ratio and the modulus of materials of low tensile resistance by the Brazilian (indirect tensile) tests with particular reference to concrete. *Australian Journal of Applied Sciences*. 10: 243-268.

Hondros, G., 1959. The Evaluation of Poisson's Ratio and the Modulus of Materials of low Tensile Resistance by the Brazilian (Indirect Tensile) Tests with Particular Reference to Concrete. *Australian Journal of Applied Sciences*. 10: 243-268.

Jaeger, J.C. & Cook, N.G.W., 1979. *Fundamentals of Rock Mechanics*. London: Chapman and Hall.

Jaeger, J.C. & Cook, N.G.W., 1979. *Fundamentals of Rock Mechanics*. London: Chapman and Hall.

Jianhong, Y., Wu, F. Q. & Sun J.Z., 2008. Estimation of Tensile Elastic Modulus using Brazilian disc by applying diametrically opposed concentrated loads. *International Journal of Rock Mechanics & Mining Sciences*.

Kenkhunthod, N. & Fuenkajorn, K., 2009. Effects of loading rate on compressive strength of sandstones under confinement. *Proceedings of the Second Thailand Rock Mechanics Symposium*, Nakhon Ratchasima: Suranaree University of Technology.

Kwaśniewski, M., Takahashi, M. & Li, X., 2003. Volume changes in sandstone under true triaxial compression conditions. *ISRM 2003–Technology Roadmap for Rock Mechanics*, South African Institute of Mining and Metallurgy.

Liao, J. J., Yang, M. T. & Hsieh, H. Y. 1997. Direct tensile behavior of a transversely isotropic rock. *International Journal of Rock Mechanics & Mining Sciences*. 34(5): 831-849.

Ohokal, M., Funatol, A. & Takahashi, Y., 1997. Tensile test using hollow cylindrical specimen. *International Journal of Rock Mechanics & Mining Sciences*. Vol. 34, No. 3-4, 1997 ISSN 0148-9062.

Oku, H., Haimson, B. & Song, S.R., 2007. True triaxial strength and deformability of the siltstone overlying the Chelungpu fault (Chi-Chi earthquake), Taiwan. *Geophysical Research Letters*. 34(9).

Reddy, K.R., Saxena, S.K. & Budiman, J.S., 1992. Development of a true triaxial testing apparatus. *Geotechnical Testing Journal*. 35(2): 89-105.

Reddy, K.R., Saxena, S.K. & Budiman, J.S., 1992. Development of a True Triaxial Testing Apparatus. *Geotechnical Testing Journal*. 15(2): 89-105.

Schwab, R. & Benz, T., 2008. a quantitative comparison of six rock failure criteria. *International Journal of Rock Mechanics and Mining Sciences*. 45: 1176-1186.

Singh, B., Goel, R.K., Mehrotra, V.K., Garg, S.K. & Allu, M.R., 1998. Effect of intermediate principal stress on strength of anisotropic rock mass. *Tunneling and Underground Space Technology*. 13: 71-79.

Smart, B. G. D., 1995. A true triaxial cell for testing cylindrical rock specimens. *International Journal of Rock Mechanics and Mining Sciences*. 32(3): 269-275.

Tepnarong, P. 2001. Theoretical and Experimental Studies to Determine Compressive and Tensile Strength of Rock, Using Modified Point Load Testing. *M.S. Thesis*, Suranaree University of Technology, Thailand.

Tiwari, R.P. & Rao, K.S., 2004. Physical modeling of a rock mass under a true triaxial stress state. *International Journal of Rock Mechanics and Mining Sciences*. 41(30):2A 141-6.

Tiwari, R.P. & Rao, K.S., 2004. Physical modeling of a rock mass under a true triaxial stress state. *International Journal of Rock Mechanics and Mining Sciences*. 41(30).

Tiwari, R.P. & Rao, K.S., 2006. Post failure behaviour of a rock mass under the influence of triaxial and true triaxial confinement. *Engineering Geology*. 84: 112-129.

Wawersik, W.R., Carlson, L.W., Holcomb, D.J. & Williams, R.J., 1997. New method for true-triaxial rock testing. *International Journal of Rock Mechanics and Mining Sciences*. 34(3-4): 365-385.

Wawersik, W.R., Carlson, L.W., Holcomb, D.J. & Williams, R.J., 1997. New method for true-triaxial rock testing. *International Journal of Rock Mechanics and Mining Sciences*. 34(330): 3-4.

Wijk, G., 1978. Some new theoretical aspects of indirect measurements of tensile strength of rock. *International Journal of Rock Mechanics & Mining Sciences*. 15: 149-160.

Yang, X. L., Zou, J. F. & SUI, Z. R., 2007. Effect of intermediate principal stress on rock cavity stability. *Journal Central South University Technology*. s1-0165-05

You, M., 2008. True-triaxial strength criteria for rock. *International Journal of Rock Mechanics and Mining Sciences*. 46: 115-127.

You, M., 2008. True-triaxial strength criteria for rock. *International Journal of Rock Mechanics and Mining Sciences*. 46: 115-127.

Effects of Intermediate Principal Stress on Compressive and Tensile Strengths of Sandstones

Paper No.298

R. Thosuwan **C. Walsri** **P. Poonprakon** **K. Fuenkajorn**
Suranaree University of technology
Nakorn Ratchasima

ABSTRACT

A series of true triaxial compression tests and indirect tension tests with axial confinements are performed to assess the effects of the intermediate principal stresses on the elasticity and strengths of three types of sandstones. These sandstones are commonly found in the north and northeast of Thailand. Their mechanical properties and responses play a significant role on the stability of the tunnels, slope embankments and dam foundations in the region. A true understanding of the failure behavior of these rocks is highly desirable. In particular, knowledge of the rock tensile strength as affected by the intermediate principal stress is rare.

Over 50 rectangular shaped specimens (50x50x100 mm) are tested using a polyaxial load frame. Lateral stresses are applied with different magnitudes between two mutually perpendicular directions ($\sigma_2 \neq \sigma_3$), and varying from 0 up to 20 MPa. The axial stress (σ_1 - along the longest axis) is increased until failure. Neoprene caps are inserted at the interfaces between loading platens and specimen surfaces to minimize the friction. The failure stresses are presented in form of octahedral shear strength (τ_{oct}) vs. mean stress (σ_m) diagram. Comparisons of the results with those obtained from the uniaxial and triaxial strength testing indicate that under the same σ_m, σ_2 can notably decrease the τ_{oct} at failure. The failure envelope is lower for the greater σ_2/σ_3 ratio. The results also indicate that the sandstones are transversely anisotropic. The elastic modulus in the direction normal to the bedding planes is about 2-4 times greater than that parallel to the bedding planes. The Poisson's ratio on the plane parallel to the beds is about three times smaller than that across the beds. These hold true for all sandstones tested here.

The effect of σ_2 on the tensile strengths is assessed by conducting the indirect tension test under confinement. The constant σ_2 with magnitudes varying from 0 to 40 MPa is applied along the axial direction of 50 mm-diameter disk samples using the polyaxial load frame. Then the line load is diametrically applied until failure occurs. The intermediate principal stress (σ_2 - axial stress in this case) significantly decreases the magnitude of the line load required to fail the disk samples. Using linear elastic theory the stress states are derived for the sample center (where the tensile crack is initiated) which is under uniaxial strain condition. A more complete failure criterion (taken σ_2 into consideration) is developed using τ_{oct} - σ_m diagram by combining the results of tension test under confinements with those of the true triaxial compression tests. The octahedral shear strengths of the rocks under the mean stresses that are lower than that obtained from the uniaxial compressive strength can be obtained.

Key Words: sandstone, true triaxial, polyaxial, intermediate principal stress, Brazilian test

BIOGRAPHY

Mr. Pakpoom Poonprakon was born on February 10, 1983 in Nakhon Ratchasima province, Thailand. He received his Bachelor's Degree in Engineering (Geotechnology) from Suranaree University of Technology in 2006. For his post-graduate, he continued to study with a Master's degree in the Geological Engineering Program, Institute of Engineering, Suranaree university of Technology. During graduation, 2006-2009, he was a part time worker in position of research assistant at the Geomechanics Research Unit, Institute of Engineering, Suranaree University of Technology. He has published two technical papers related to rock mechanics, titled **"Compressive and Tensile Strengths of Sandstones under True Triaxial Stresses"** published in the Proceeding of the Second Thailand symposium on rock mechanics, Chonburi, Thailand; and **"Effects of Intermediate Principal on Compressive and Tensile Strengths of Sandstones"** in the Proceeding of International Symposium on Rock Mechanics, University of Hong Kong, Hong Kong. For his work, he is a good knowledge in geomechanics theory and practice.